J. Micropalaeontology, 43, 303–322, 2024
https://doi.org/10.5194/jm-43-303-2024

Journal of Micropalaeontology
Open Access

Transient micropaleontological turnover across a late Eocene (Priabonian) carbon and oxygen isotope shift on Blake Nose (NW Atlantic)

Julia de Entrambasaguas[1,2], Thomas Westerhold[3], Heather L. Jones[3], and Laia Alegret[1,2]

[1]Departamento de Ciencias de la Tierra, Universidad de Zaragoza, 50009 Zaragoza, Spain
[2]Instituto Universitario de Ciencias Ambientales de Aragón, Universidad de Zaragoza, 50009 Zaragoza, Spain
[3]MARUM – Center for Marine Environmental Sciences, University of Bremen, 28359 Bremen, Germany

Correspondence: Julia de Entrambasaguas (jdeentrambasaguas@unizar.es)

Received: 1 December 2023 – Revised: 27 May 2024 – Accepted: 10 June 2024 – Published: 8 August 2024

Abstract. The Gulf Stream, a western boundary current transporting warm water into the North Atlantic, plays a key role in climate regulation and oceanographic stability at a regional and global scale as part of the Atlantic Meridional Overturning Circulation (AMOC). Evidence suggests that an ancestral Gulf Stream has existed since the Mesozoic, and it has altered its course repeatedly over Cenozoic times. In this study, we focus on the upper Eocene (Priabonian, ca. 36 Ma) from Ocean Drilling Program Site 1053 on Blake Nose (subtropical North Atlantic). Bulk carbon and oxygen stable isotopes, as well as benthic foraminiferal and calcareous nannofossil assemblages, provide an integrated assessment of the palaeoceanographic changes impacting the area through the water column to the seafloor. Micropaleontological assemblages suggest changes in surface ocean stratification and nutrient supply to the seafloor coeval with a paired negative carbon and oxygen isotope excursion and the return to background conditions higher up in the study section. These transitory changes are compatible with the longitudinal displacement of the proto-Gulf Stream and its related eddies. Our results build on previous work and support the hypothesis that links palaeoceanographic changes in the Blake Nose area with shifts in the proto-Gulf Stream during the middle and late Eocene.

1 Introduction

The middle to late Eocene was marked by significant global changes, including progressive cooling, lower-atmospheric CO_2, the formation of permanent ice sheets in Antarctica, and the reorganization of deep-ocean currents (Zachos et al., 1994; Lear et al., 2000; Cramer et al., 2009; Borrelli et al., 2014, 2021; Agnostou et al., 2016; Cramwinckel et al., 2018; Westerhold et al., 2020). Regional palaeogeography deeply impacted ocean circulation during this time, with the transition towards a heterogeneous circulation model linked to the opening of circumpolar passages near the Southern Ocean ca. 35 Ma (Cramer et al., 2009; Borrelli et al., 2014, 2021; Hutchinson et al., 2018). In contrast, the flow of the Gulf Stream was driven by sharp temperature gradients (Gordon, 1991).

The subtropical North Atlantic Ocean was characterized by high palaeoproductivity (Borrelli et al., 2014, 2021; Witkowski et al., 2021) and volatile palaeoceanographic conditions (Wade et al., 2000, 2001; Wade and Kroon, 2002) during the middle to late Eocene. Enhanced primary production in the area has been linked to the influence of the circumglobal Tethyan current, which delivered nutrient-rich deep waters to the low latitudes (Hotinski and Toggweiler, 2003) and reallocated nutrients towards the subtropics via Ekman transport (Bice et al., 2000; Huber and Sloan, 2000; Borrelli et al., 2021). Geochemical data (e.g. Wade and Kroon, 2002; Okafor et al., 2009) have suggested strong and rapid fluctuations in the sea surface temperature (SST) and an unstable water column structure since the middle Eocene. This particular palaeoceanographic setting had a significant impact on planktic taxa, with faunal turnovers reflecting shifts in nutrient availability and rapid changes in the SST (Boersma

et al., 1987; Guernet and Bellier, 2000; Van Mourik et al., 2001; Kamikuri and Wade, 2012). Nevertheless, the underlying mechanisms driving these changes have been a matter of debate, with proposed explanations including changes in upwelling intensity (Wade et al., 2000), a latitudinal displacement of the proto-Gulf Stream (Wade and Kroon, 2002), and fluctuations on the distribution of its associated eddies (Okafor et al., 2009).

The Gulf Stream is a fast, narrow current that mobilizes warm water from the Gulf of Mexico into the subtropical North Atlantic Gyre, which is critical in transferring heat to the eastern North Atlantic Ocean and western Europe (Gordon et al., 1991). The temperature contrast between the warm water transported by the Gulf Stream and the colder surrounding waters favours the formation of meanders which turn into eddies after disengaging from the main stream (Richardson, 1983; Dewar and Flierl, 1987). They then drift apart, disrupting water column stratification for up to several hundreds of kilometres as they move westward (Fuglister, 1972; Richardson, 1983). Climate modelling suggests that an ancestral Gulf Stream has existed since the late Maastrichtian (∼ 68 Ma) (Watkins and Self-Trail, 2005). According to seismic stratigraphy data (Pinet et al., 1981), this proto-Gulf Stream altered its course several times during the Paleogene, possibly causing drastic changes in sea surface temperatures and salinity at a regional scale (Wade and Kroon, 2002). Overall, palaeoceanographic reconstructions of the subtropical North Atlantic Ocean have focused on the middle Eocene (e.g. Wade et al., 2001), with an emphasis on the upper middle Eocene (∼ 37.3–39.6 Ma) (Wade et al., 2000; Wade and Kroon, 2002; Okafor et al., 2009; Kamikuri and Wade, 2012), but late Eocene reconstructions are relatively scarce (Katz et al., 2011; Borrelli et al., 2014, 2021). Moreover, most of these studies are based on water column proxies and planktic biota, leaving the response of the benthos to climatic and oceanographic changes largely unexplored.

Benthic foraminifera are the most common meiofaunal, unicellular deep-sea biota forming external skeletons (tests). Along with bottom-water temperature and oxygenation levels, the flux of organic matter from the surface to the deep ocean is one of the main factors shaping the community composition of benthic foraminifera (e.g. Gooday, 1993; Thomas et al., 1995; Sun et al., 2006), with both the nature of the organic matter and the intensity and regularity of its delivery to the seafloor having a strong influence (e.g. Gooday, 1993; Smart et al., 1994; Gooday and Hughes, 2002). The delivery of phytodetritus (i.e. detrital material consisting of phytoplankton and zooplankton remains bound together by a gelatinous matrix; Gooday and Turley, 1990) to the seafloor has been proposed as an important pathway for carbon deposition in the western North Atlantic (Billett et al., 1983; Rice et al., 1986; Thiel et al., 1989), as well as in other areas (Gooday and Turley, 1990; Smart et al., 1994; Jorissen and Wittling, 1999). Benthic foraminiferal assemblages respond rapidly to changes in their environment, which makes them excellent proxies for oxygenation and nutrient availability in the deep sea (e.g. Bernhard and San Gupta, 1999; Murray, 2006). Therefore, their interpretation is key in addressing how global- and regional-scale phenomena affect palaeoenvironmental and palaeoecological conditions at the seafloor (e.g. Alegret et al., 2021a).

In this study, we investigate the expression of changes in the proto-Gulf Stream distribution within both the planktic and benthic realms during the late Eocene (∼ 36 Ma) at Ocean Drilling Program (ODP) Site 1053 (Blake Nose in the subtropical North Atlantic Ocean). Stable isotope data measured on bulk sediment, combined with quantitative and semi-quantitative analyses of benthic foraminiferal and calcareous nannofossil assemblages, respectively, reveal the evolution of primary productivity, water stratification, and seafloor nutrient availability in the Blake Nose area. We also identify a transient negative shift in the carbon and oxygen stable isotope records and explore its relationship with possible alterations to the course of the proto-Gulf Stream.

2 Material and methods

2.1 Location and setting

ODP Site 1053 was drilled during Leg 171B at the top of the Blake escarpment (29°59.538′ N, 76°31.413′ W; 1629.5 m water depth) in the western North Atlantic Ocean (Fig. 1). The Blake Plateau began its formation as the African and North American plates started disengaging in the Late Triassic (Murphy, 1995). Its topography has been strongly influenced by the activity and fluctuations in the Gulf Stream, which is also the case for the adjacent Hatteras continental slope (Paull and Dillon, 1980). For most of the Late Jurassic and Early Cretaceous, the Blake Plateau was the site of shallow-water carbonate deposition (Schlagintweit and Enos, 2013). By the middle–late Eocene, ODP Site 1053 reached an estimated palaeodepth of 1500–1750 m (Katz et al., 2011). Sedimentation rates during the latest middle and late Eocene are notably high for an open-pelagic setting (Katz et al., 2011; Borrelli et al., 2021). High-carbonate accumulation rates through the middle to late Eocene have been linked to remarkable biogenic input from the euphotic zone up until ∼ 35 Ma when they suddenly plummet, reflecting either a disconformity with a ∼ 1 Ma hiatus or an abrupt halt in sediment accumulation (Borrelli et al., 2021).

Paleogene and Cretaceous materials in the Blake Nose area have never been fully covered by younger sediments and are barely affected by diagenesis (Wade et al., 2000). Site 1053 contains a fairly complete sequence of mid- and late Eocene sediments (Norris et al., 1998). The good preservation of the sequence, composed of nannofossil ooze intercalated with some levels of siliceous nannofossil ash, is reflected by the well-preserved microfossil assemblages.

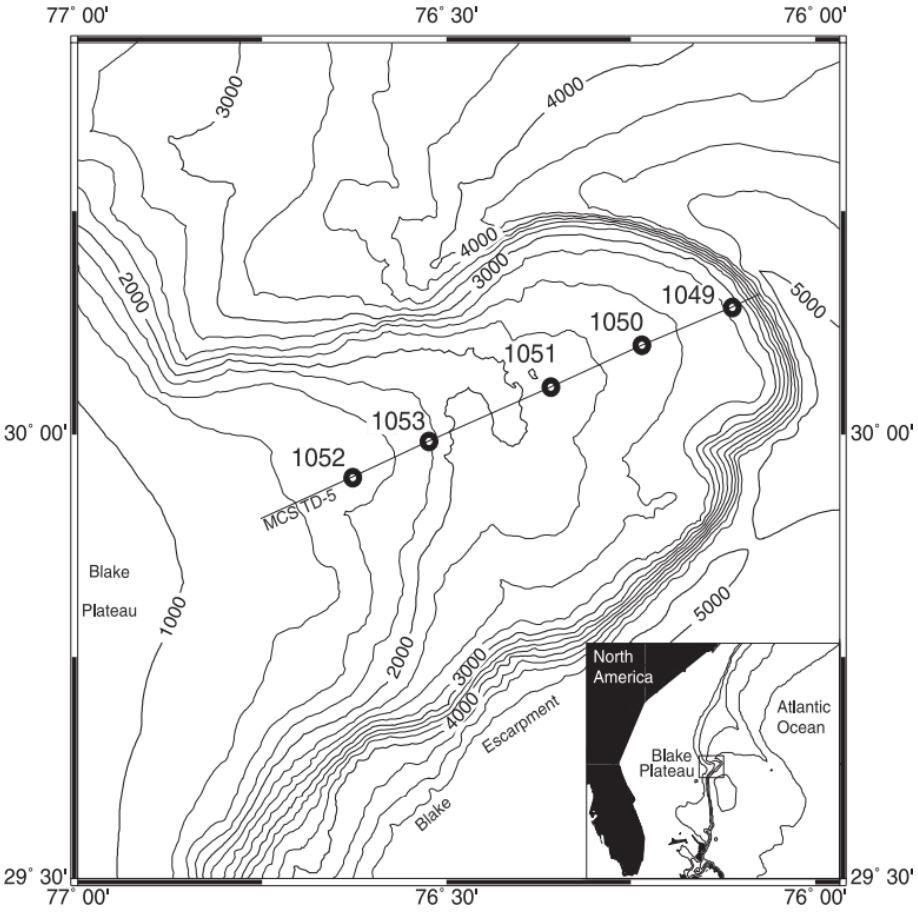

Figure 1. Geographical location and depth (m) of Ocean Drilling Program Leg 171B, including ODP Site 1053 in the subtropical North Atlantic Ocean (Kroon et al., 1998).

2.2 Sediments and sampling

The shipboard biostratigraphy of Hole 1053B reveals a stratigraphically expanded upper Eocene section represented in Cores 1H through 17X (~0 to 150 m b.s.f.; Norris et al., 1998). In this study, we focus on a very short, 70 cm thick interval within Core 8H section 5, where preliminary data revealed intriguing, transient shifts in the carbon and oxygen stable isotope records that may be related to palaeoceanographic and/or palaeoclimatic alterations. The sediment from this core section is a greenish-grey nannofossil ooze with some darker, clay-rich layers. Bioturbation is light to moderate, with pyrite occurring most commonly in the burrows (Norris et al., 1998).

Samples were taken every centimetre between Site 1053B Core 8H-5W, 7.5–8.5 cm, and Core 8H-5W, 77.5–78.5 cm (66.98–67.68 m b.s.f., below sea floor), at the International Ocean Discovery Program Bremen Core Repository (BCR) in the MARUM – Center for Marine Environmental Sciences (University of Bremen). Samples had previously been taken between 42.5 and 44.5 cm in Hole B, Section 1053B-8H-5W, motivating the substitution of this interval with Hole A, Core 8H (Section 2), at 69.5 to 71.5 cm (68.70–68.72 m b.s.f.), which is contemporaneous based on a revised composite record developed using X-ray fluorescence core scanning data (unpublished, Thomas Westerhold, personal communication, 2021). For the scope of this study, the composite record is not critical as samples come from two well-correlated sections. For consistency from now on, we refer to the revised metre composite depth (rmcd) scale but report all data with the full sample location to allow reproducibility.

2.3 Stable isotope analyses

Stable carbon ($\delta^{13}C$) and oxygen ($\delta^{18}O$) isotope analyses were performed on 70 bulk sediment samples (at a 1 cm sampling resolution) across the study interval (74.5–75.20 rmcd). The analyses were conducted at MARUM Isotope Laboratory (Bremen University) using a Finnigan MAT 251 gas isotope ratio mass spectrometer with Kiel I automated carbonate preparation device. Data are registered relative to the Vienna Pee Dee Belemnite (VPDB) international standard determined by adjustment to a calibrated in-house standard (Solnhofen limestone). The deviation of the house stan-

dard over the measurement period was 0.04 ‰ for $\delta^{13}C$ and 0.05 ‰ for $\delta^{18}O$.

2.4 Benthic foraminiferal analyses

Quantitative analyses of benthic foraminiferal assemblages were performed on a subset of 26 samples between 74.54 and 75.20 rmcd. Sample selection was made following preliminary results on stable isotopes to cover background values, as well as the negative shifts in $\delta^{13}C$ and $\delta^{18}O$, with a resolution that ranges from 1 to 10 cm. Samples were oven-dried (< 50 °C for 24 h), weighed, and soaked in $NaPO_3)_6$ for 3 h. Disaggregated samples were sieved under running water with a 63 µm mesh size sieve. The > 63 µm size fraction was collected, oven-dried (< 50 °C for 24 h), and weighed again. For each sample, around 300 specimens were picked as a representation of the assemblage. A total of 73 taxa (68 calcareous and 5 agglutinated) were identified at the species or higher taxonomic levels. Classification at the genus level mainly follows Loeblich and Tappan (1987). Species identification follows Van Morkhoven et al. (1986), Fenero et al. (2010), Holbourn et al. (2013), and Boscolo-Galazzo et al. (2015).

Preservation of benthic foraminifera is generally good at Site 1053, and some of the most representative specimens were photographed at the scanning electron microscope (SEM) imaging facilities at the University of Zaragoza (Spain) (Plate 1). The relative abundance of each taxon was calculated from the raw data matrix that contains the original assemblage counts (Table 1). All taxa that make up > 2 % of the assemblages in at least one sample are represented in Fig. 2. The percentage of calcareous and agglutinated tests was calculated, and the diversity (Fisher's α index) and heterogeneity (Shannon–Weaver $H(S)$ index) of the assemblages were calculated following Murray (2006) (Fig. 3). The percentage of the buliminids sensu *lato* (s.l.) group was calculated following Alegret and Thomas (2013) and Alegret et al. (2021a). Taxa were assigned to infaunal or epifaunal morphogroups according to their morphology, following Corliss (1985) and Corliss and Chen (1988). The TROX model (Jorissen et al., 1995) was applied to infer oxygenation and food supply to the seafloor based on the microhabitat distribution of fossil benthic foraminifera (e.g. Jorissen et al., 1995). Note that the allocation of foraminifera to microhabitats may be inaccurate because some taxa are not static but actively move through the sediment (e.g. Fontanier et al., 2002) and because the relative role of organic matter availability and dissolved oxygen is debated (e.g. Bouchet et al., 2009; Mallon et al., 2012; Singh et al., 2021).

2.5 Calcareous nannofossil analyses

Nannofossil smear slides were prepared from the same sediments used for the stable isotope and benthic foraminiferal analyses (depth interval of 74.54–75.20 rmcd), following the standard methods of Bown and Young (1998). A subset of 26 samples (selected to capture both background values and the negative shifts in $\delta^{13}C$ and $\delta^{18}O$) was then examined using an Olympus BX51 polarizing microscope at the MARUM – Center for Marine Environmental Sciences (University of Bremen). Biostratigraphic analyses were conducted at low (600×) magnification along two long transects of each slide to ensure that rare, biostratigraphically significant taxa were not overlooked. All nannofossils were identified to species level using the taxonomic concepts compiled in the Nannotax 3 online database (Young et al., 2022), and the biozonation scheme of Agnini et al. (2014) was applied.

For qualitative assemblage analyses, 10 fields of view (FOV) from a representative area of each slide were examined at higher (1000×) magnification. The individual abundance of each species within a sample was then estimated as follows:

C, with at least one specimen present in every FOV;

Fr, with one specimen present in five to nine of the FOV;

F, with one specimen present in two to five of the FOV;

R, with a specimen only present in one of the FOV; and

VR, with five or fewer specimens observed within the whole sample (used for the taxa that were only observed while conducting biostratigraphic analyses).

To better evaluate how the nannofossil community composition varied throughout the study interval, we conducted a principal component analysis (PCA) (Fig. 4). Because a numerical matrix is required for multivariate statistics, each of the discrete categories outlined above were allocated a number from 1 to 5 (for the VR, R, F, Fr, and C categories, respectively). A value of zero was assigned if a species was not observed within a sample. A PCA was then conducted on the resultant matrix using the "prcomp" function in R, and the results were visualized using the factoextra package.

3 Results

3.1 Calcareous nannofossil biostratigraphy

The original age model for the late Eocene of ODP Site 1053 is based on the shipboard data (Norris et al., 1998) which indicates that the study interval is located in the upper Eocene calcareous nannofossil Subzone CP15b (base *Isthmolithus recurvus*; Okada and Bukry, 1980). Since then, significant advances have been made in Paleogene nannofossil biozonation, including the replacement of unreliable marker taxa (e.g. *I. recurvus*) with those that have a relatively more robust biostratigraphic signal (e.g. species belonging to the genus *Reticulofenestra*/*Cribrocentrum*; Raffi et al., 2016). According to these newer biozonation schemes,

Table 1. Relative abundance of benthic foraminifera from ODP Site 1053.

Depth (m b.s.f.)	67.02	67.07	67.12	67.17	67.22	67.27	67.36	67.38	67.40	67.42	67.43	67.44	67.45	67.46	67.4725	67.48	67.49	67.50	67.51	67.52	67.53	67.58	67.64	67.68
Depth (rmcd)	74.54	74.59	74.64	74.69	74.74	74.79	74.88	74.9	74.92	74.94	74.95	74.96	74.97	74.98	74.993	75	75.01	75.02	75.03	75.04	75.05	75.1	75.16	75.2
Taxa/sample	1053B8H5-5	1053B8H5-10	1053B8H5-15	1053B8H5-20	1053B8H5-25	1053B8H5-30	1053B8H5-39	1053B8H5-41	1053B8H5-43	1053B8H5-45	1053B8H5-46	1053B8H5-47	1053B8H5-48	1053B8H5-49	1053B8H5-50b	1053B8H5-51	1053B8H5-52	1053B8H5-53	1053B8H5-54	1053B8H5-55	1053B8H5-56	1053B8H5-61	1053B8H5-67	1053B8H5-71
Ammodiscus sp.	0.00	0.00	0.29	0.00	0.00	0.00	0.00	0.00	0.00	0.00	0.00	0.00	0.00	0.00	0.00	0.00	0.00	0.00	0.00	0.00	0.00	0.00	0.00	0.00
Angulogerina muralis	0.00	0.92	0.00	0.00	0.00	0.32	0.00	0.00	0.00	0.00	0.67	0.00	0.00	0.00	0.33	0.00	0.00	0.67	0.00	0.00	0.00	0.00	0.00	1.06
Angulogerina sp.	0.00	0.00	0.00	0.00	0.33	0.32	1.35	1.37	0.33	0.00	0.00	0.00	1.34	0.71	0.33	0.63	0.39	0.67	0.00	0.00	0.00	1.32	0.00	0.35
Anomalinoides spissiformis	0.00	0.92	1.16	0.00	0.00	0.00	0.68	0.00	0.00	0.00	0.00	0.00	0.00	1.79	0.00	0.00	0.00	0.00	0.00	0.00	0.00	0.00	0.00	0.00
Anomalinoides spp.	2.03	0.31	3.77	3.44	3.67	2.91	1.01	0.00	0.99	2.12	2.01	2.32	2.68	3.57	2.28	2.51	1.16	0.67	1.42	1.00	0.73	0.99	2.15	0.35
Aragonia aragonensis	0.00	0.00	0.00	0.34	0.00	0.00	0.00	0.00	0.00	0.00	0.00	0.00	0.00	0.00	0.00	0.00	0.00	0.33	0.00	0.00	0.00	0.00	0.00	0.00
Bolivina spp.	0.00	0.00	0.00	1.37	1.00	0.00	0.00	0.00	0.33	0.00	0.67	0.33	0.00	0.36	0.65	0.00	0.00	0.00	0.00	0.00	0.00	2.31	0.00	0.00
Bolivinoides sp.	1.01	0.00	1.16	3.78	0.00	0.97	0.00	1.71	0.99	0.00	0.33	0.00	0.45	0.00	0.00	0.31	0.77	0.00	1.07	0.67	0.36	0.66	0.00	0.00
Brizalina sp.	3.04	3.98	1.74	2.06	3.67	3.88	2.70	3.07	5.94	3.18	4.01	3.97	5.36	4.64	3.91	1.88	4.63	4.33	4.27	3.67	3.64	4.29	5.15	3.90
Brizalina tectiformis	6.08	9.17	5.80	3.09	4.67	5.50	5.07	6.48	4.95	3.89	4.68	4.97	8.04	5.36	5.21	6.58	9.65	5.00	3.20	3.33	4.36	4.62	3.00	2.48
Bulimina alazanensis	0.00	3.98	0.29	0.34	0.00	0.00	0.00	0.00	0.00	1.06	0.00	1.32	0.45	0.00	0.00	0.00	0.00	0.00	0.00	0.00	0.36	0.00	0.00	0.35
Bulimina elongata	0.00	0.00	0.00	0.00	2.67	0.00	0.00	0.00	0.00	0.35	0.33	0.99	0.00	0.71	0.33	0.63	0.00	0.00	0.00	0.00	0.00	0.00	0.00	0.00
Bulimina simplex	1.01	0.00	0.00	0.00	0.00	0.00	0.00	0.00	0.00	0.00	0.00	0.00	0.00	0.00	0.00	0.00	0.00	0.00	0.00	0.00	0.00	0.00	0.00	1.06
Bulimina spp.	0.68	0.00	0.58	0.00	0.00	2.27	0.68	0.00	0.00	0.71	0.67	1.99	0.45	1.07	0.65	0.31	0.00	0.00	1.07	0.67	0.00	0.33	0.00	0.71
Bulimina truncana	0.00	0.31	0.00	0.00	0.00	0.65	0.00	0.00	0.00	0.00	0.00	0.00	0.00	0.00	0.00	0.00	0.00	0.00	0.00	0.00	0.00	0.00	0.00	0.00
Bulimina tuxpamensis	0.00	0.00	0.00	0.00	0.00	0.00	0.00	0.00	0.00	0.00	0.00	0.00	0.00	0.00	0.00	0.31	0.00	0.33	0.36	0.00	0.00	0.00	0.00	0.00
Buliminella spp.	0.00	0.31	0.00	0.00	0.00	0.00	0.00	0.00	0.00	0.00	0.00	0.00	0.00	0.00	0.00	0.00	0.00	0.00	0.00	0.00	0.00	0.00	0.00	0.00
Cassidulina crassa	2.36	6.73	0.00	0.00	4.33	1.29	2.36	2.05	2.31	1.06	0.33	0.33	2.23	1.43	0.65	1.57	0.00	0.00	1.07	0.67	0.00	0.33	0.00	2.84
Cassidulina spp.	0.34	0.00	2.61	0.34	0.00	0.00	0.00	0.00	0.00	0.00	0.00	0.00	0.00	0.36	0.00	0.94	0.00	1.33	0.36	2.00	0.73	2.31	0.00	0.00
Chillostomella oolina	0.00	0.00	0.00	0.00	0.00	0.00	0.00	0.00	0.00	0.00	0.00	0.00	0.45	0.00	0.00	0.00	0.00	0.00	0.00	0.00	0.00	0.00	0.00	0.35
Chillostomella spp.	0.00	0.00	0.00	0.00	0.00	0.00	0.00	0.00	0.33	0.00	0.00	0.00	0.00	0.00	0.00	0.00	0.00	0.00	0.00	0.00	0.00	0.00	0.00	0.00
Cibicides lobatulus	0.00	0.31	2.03	0.69	0.00	0.00	0.00	0.00	0.00	0.00	0.00	0.00	1.79	1.79	2.61	1.57	1.16	0.33	2.85	4.00	4.00	1.65	1.72	0.00
Cibicides spp.	0.00	0.00	0.29	0.00	0.00	0.00	0.00	0.00	0.00	0.00	0.00	0.66	0.00	0.00	0.00	0.00	0.39	0.00	0.00	0.00	0.00	0.00	0.00	0.00
Cibicidoides eocaenus	0.00	3.06	0.00	0.00	3.67	2.91	1.69	0.34	0.99	0.35	1.00	1.32	1.34	0.71	0.00	0.00	0.00	0.00	0.00	0.00	0.00	0.00	0.00	0.71
Cibicidoides micrus	0.00	0.00	0.58	0.69	0.00	1.94	0.34	0.68	0.00	0.00	0.00	0.33	0.00	0.00	0.00	0.31	0.00	0.33	0.36	0.33	0.00	0.00	0.00	0.00
Cibicidoides spp.	3.04	2.45	1.45	5.50	4.67	3.24	6.08	5.12	3.63	5.30	5.02	3.97	6.70	6.79	6.84	4.39	1.16	4.00	3.56	2.67	3.27	2.97	5.15	1.77
Evolvocassidulina spp.	0.00	0.00	0.00	0.00	0.00	0.32	0.00	0.00	0.33	0.35	0.00	0.00	0.00	0.00	0.00	0.00	0.00	0.00	0.00	0.00	0.00	0.00	0.00	0.00
Fissurina sp.	0.00	0.00	0.00	0.00	0.00	0.00	0.00	0.00	0.00	0.00	0.00	0.00	0.00	0.00	0.33	0.00	0.00	0.00	0.00	0.00	0.00	0.00	0.00	0.35
Fursenkoina spp.	0.00	0.00	0.00	0.69	3.00	0.32	0.00	0.00	0.33	1.06	0.00	0.00	1.34	0.36	0.33	0.00	0.77	0.00	0.36	0.00	1.09	0.00	0.43	0.00
Globocassidulina spp.	0.00	0.00	0.29	0.00	2.00	0.00	0.00	1.02	0.66	2.12	2.01	1.66	1.79	2.50	2.28	2.51	2.32	0.00	2.49	1.67	1.82	0.33	0.00	1.06
Globocassidulina subglobosa	10.81	11.01	7.54	11.34	3.00	3.88	4.05	5.80	6.60	7.07	7.02	6.95	7.59	6.79	9.77	4.70	7.72	5.67	4.98	5.33	6.91	6.60	0.00	6.38
Globulina sp.	0.00	0.00	0.00	0.00	0.00	0.00	0.00	0.00	0.00	0.00	0.00	0.00	0.00	0.00	0.00	0.00	0.00	0.00	0.36	0.33	0.36	0.00	0.00	0.00
Gyroidinoides planulatus	0.00	0.92	0.00	0.00	0.67	0.00	0.00	2.05	0.00	1.77	1.00	0.66	0.89	0.36	0.00	1.88	0.00	0.00	1.07	1.33	1.09	0.00	0.86	1.06
Gyroidinoides spp.	1.69	0.61	3.48	0.69	0.00	1.29	3.04	1.02	2.97	2.47	1.34	3.64	1.34	1.43	0.98	2.19	0.77	2.33	1.78	2.00	0.73	0.66	1.29	1.42
Hanzawaia ammophila	0.00	0.31	0.00	0.00	0.33	0.00	0.00	0.00	0.00	0.00	0.00	0.00	0.00	0.36	0.00	0.00	0.00	0.00	0.00	0.00	0.00	0.00	0.00	0.00
Hanzawaia spp.	0.00	0.00	0.00	0.00	0.00	0.00	0.00	0.00	0.00	0.00	0.33	0.00	0.00	0.00	0.65	0.00	0.00	0.00	0.00	0.00	0.00	0.00	0.00	0.00
Heronallenia lingulata	0.00	0.31	0.29	0.69	0.00	0.00	0.34	0.00	0.00	0.00	0.00	0.00	0.00	0.00	0.00	0.00	0.00	0.00	0.00	0.00	0.00	0.00	0.86	0.35
Lagena spp.	0.00	0.00	0.00	0.00	0.33	0.00	0.00	0.34	0.00	0.00	0.00	0.00	0.45	0.00	0.00	0.31	0.00	0.00	0.36	0.00	0.73	0.00	1.72	0.00
Lenticulina spp.	0.34	1.83	1.16	1.03	0.00	1.62	0.00	0.34	0.66	0.35	0.33	0.33	0.00	1.07	2.61	0.94	0.00	0.33	0.71	0.00	0.73	0.00	0.00	0.35

https://doi.org/10.5194/jm-43-303-2024

Table 1. Continued.

Depth (m b.s.f.)	67.02	67.07	67.12	67.17	67.22	67.27	67.36	67.38	67.40	67.42	67.43	67.44	67.45	67.46	67.4725	67.48	67.49	67.50	67.51	67.52	67.53	67.58	67.64	67.68
Depth (rmcd)	74.54	74.59	74.64	74.69	74.74	74.79	74.88	74.9	74.92	74.94	74.95	74.96	74.97	74.98	74.993	75	75.01	75.02	75.03	75.04	75.05	75.1	75.16	75.2
Taxa/sample	1053B8H5-5	1053B8H5-10	1053B8H5-15	1053B8H5-20	1053B8H5-25	1053B8H5-30	1053B8H5-39	1053B8H5-41	1053B8H5-43	1053B8H5-45	1053B8H5-46	1053B8H5-47	1053B8H5-48	1053B8H5-49	1053B8H5-50b	1053B8H5-51	1053B8H5-52	1053B8H5-53	1053B8H5-54	1053B8H5-55	1053B8H5-56	1053B8H5-61	1053B8H5-67	1053B8H5-71
Melonis barleeanum	0.00	1.22	0.00	0.00	0.00	0.00	0.00	0.00	0.33	1.06	0.00	1.32	0.45	0.00	0.00	0.00	0.00	0.00	0.00	0.00	0.00	0.00	0.00	0.00
Nodosariid	0.68	1.83	0.58	0.34	0.00	0.65	1.35	0.00	0.33	0.71	1.00	0.00	2.23	0.36	0.98	0.63	0.39	1.67	0.36	0.00	1.45	0.99	0.00	1.06
Nonion havanense	0.00	0.92	0.00	0.00	0.00	0.00	0.00	0.00	0.00	0.00	0.00	0.00	0.89	0.00	0.33	0.31	0.00	0.00	0.00	0.00	0.00	0.00	0.43	0.35
Nonion spp.	0.00	0.00	0.00	0.69	0.00	0.00	0.00	0.00	0.00	0.00	0.00	0.00	0.00	1.07	0.00	0.31	0.39	0.33	0.00	0.00	0.00	0.00	0.43	0.35
Nonionella robusta	1.01	0.92	0.29	1.37	1.33	0.65	0.34	2.39	1.65	0.71	1.00	1.32	1.79	0.71	1.30	0.94	0.00	1.00	1.42	1.00	1.82	1.32	0.43	0.35
Nonionella sp.	0.00	0.00	0.87	0.34	2.33	0.65	1.69	1.02	0.33	1.41	0.00	0.99	1.34	0.71	0.00	0.63	0.00	0.33	1.07	0.33	1.45	0.33	0.43	0.71
Nuttallides spp.	2.36	3.67	3.48	2.06	2.00	3.88	0.68	0.68	2.31	3.18	3.01	2.65	0.45	0.71	1.63	0.63	0.39	3.67	2.14	1.67	1.09	3.30	2.58	1.06
Nuttallinella spp.	0.00	0.00	3.48	1.37	1.33	0.00	1.01	0.00	3.30	4.24	9.70	4.97	5.36	6.79	1.30	1.25	5.41	1.33	6.41	5.33	9.09	3.63	8.15	1.42
Oridorsalis umbonatus	0.34	0.31	0.87	0.69	0.00	0.65	0.34	0.00	0.00	0.00	0.00	0.00	0.00	0.00	0.00	0.63	0.39	0.67	0.36	0.00	0.00	0.33	0.00	1.42
Osangularia spp.	0.00	0.00	0.00	0.00	0.00	0.32	0.00	0.00	0.00	0.35	0.33	0.00	0.45	0.36	0.00	0.63	0.00	0.33	0.36	0.00	0.36	0.00	0.00	0.00
Patellina spp.	0.00	0.00	0.00	0.69	0.00	0.32	0.68	0.68	0.00	0.35	0.33	0.33	0.00	0.00	0.00	0.63	0.00	0.00	1.07	0.33	0.73	0.33	0.00	0.00
Planulina spp.	0.34	0.00	0.29	0.34	0.00	0.00	0.00	0.00	0.66	0.35	0.67	0.33	0.00	0.36	0.00	0.00	0.00	0.67	0.00	0.00	0.36	0.99	0.43	1.06
Pleurostomella sp.	1.01	0.61	0.00	0.69	0.67	1.29	0.00	1.02	0.00	1.41	1.00	0.33	0.45	0.36	0.33	0.00	0.39	0.33	0.71	0.00	0.36	0.33	1.72	0.00
Polymorphinids	0.00	0.00	0.29	0.34	0.33	0.00	1.69	0.68	0.00	0.71	0.33	0.33	0.00	0.00	0.33	0.00	0.00	0.00	0.00	0.00	2.18	0.00	0.00	0.35
Praebulimina sp.	0.00	0.00	0.00	0.00	0.00	0.00	0.00	0.00	0.00	0.00	0.00	0.00	0.00	0.00	0.00	0.00	0.00	0.00	0.00	0.00	0.00	0.00	0.00	1.06
Pseudoparella spp.	59.80	38.23	50.43	42.61	45.33	48.54	46.96	53.24	45.87	39.58	36.45	40.07	26.34	34.64	36.81	46.08	50.58	51.33	44.48	53.67	39.64	45.87	50.64	53.19
Pseudouvigerina sp.	0.00	0.00	0.00	0.00	0.00	0.00	0.00	0.00	0.00	0.00	0.00	0.00	0.00	0.00	0.33	0.00	0.00	0.00	0.00	0.00	0.00	0.00	0.00	0.00
Pullenia bulloides	0.00	0.61	0.29	0.00	1.33	0.00	0.00	0.00	0.00	0.00	0.33	0.00	0.45	0.71	0.33	0.00	0.00	0.00	0.71	0.33	0.36	0.33	0.00	0.00
Pullenia quinqueloba	0.34	0.31	0.00	0.34	0.00	0.00	0.00	0.00	0.00	0.71	1.00	0.33	0.00	0.00	0.00	0.00	0.00	0.67	0.00	0.00	0.00	0.00	0.00	0.00
Pullenia spp.	0.00	0.00	0.00	0.00	0.00	0.00	0.00	0.34	0.33	0.00	0.00	0.00	0.00	0.00	0.00	0.00	0.00	0.00	0.00	0.00	0.00	0.00	0.00	0.00
Pyramidina sp.	0.00	0.00	0.29	2.41	0.00	0.32	0.00	1.02	1.98	1.77	2.34	0.66	0.89	0.36	3.58	0.63	1.16	2.00	1.42	1.67	1.09	2.31	2.15	1.42
Quadrimorphina allomorphinoides	0.00	0.00	0.29	0.00	0.67	0.00	0.34	0.00	0.00	0.00	0.00	0.66	0.45	0.00	0.00	0.00	0.00	0.00	0.00	0.00	0.36	0.00	0.00	0.00
Quadrimorphina sp.	0.00	0.00	0.58	0.00	0.00	0.00	0.00	0.00	0.00	0.00	0.00	0.00	0.45	0.00	0.00	0.63	0.00	0.00	0.36	0.00	0.00	0.00	0.00	0.35
Rhabdammina sp.	0.34	0.00	0.29	0.34	0.33	0.32	0.68	0.00	0.33	0.00	0.67	0.33	0.00	0.36	0.65	0.63	1.16	0.33	0.71	0.00	0.00	0.00	0.00	0.00
Rhizammina spp.	0.68	0.31	0.29	0.34	0.00	0.65	0.68	0.34	0.00	0.00	0.00	0.00	0.00	0.00	0.33	0.31	0.77	0.00	0.00	0.00	0.36	0.00	0.43	0.00
Spiroplectammina sp.	0.00	0.00	0.58	0.69	0.67	0.65	0.00	0.34	0.66	1.06	0.67	0.99	1.79	1.07	0.65	0.63	0.39	0.33	0.71	0.00	0.36	0.33	0.00	0.00
Stainforthia spp.	0.00	0.00	0.87	4.47	0.00	1.94	3.04	1.71	2.97	1.77	2.01	1.66	2.23	2.50	1.95	2.82	2.32	3.00	2.14	2.67	4.00	4.95	5.15	3.55
Stillostomella sp.	0.34	1.22	0.58	0.00	0.67	0.97	1.01	0.68	1.65	1.77	2.68	1.99	2.23	1.07	1.30	1.57	0.39	1.00	0.00	0.00	0.00	1.65	0.43	0.00
Tappanina selmensis	0.00	0.00	0.00	0.00	0.33	0.00	0.00	0.00	0.00	0.00	0.00	0.00	0.00	0.00	0.00	0.00	0.00	0.00	0.00	0.00	0.00	0.00	0.00	0.00
Tappanina spp.	0.00	0.00	0.00	0.00	0.00	0.00	0.00	0.00	0.00	0.00	0.00	0.00	0.45	0.00	0.00	0.00	0.00	0.00	0.00	0.00	0.00	0.00	0.00	0.00
Turrillina brevispira	0.00	0.00	0.29	0.00	0.00	0.00	0.34	0.00	0.33	0.00	0.00	0.00	0.89	0.36	0.33	0.31	0.39	0.00	0.36	0.33	0.36	0.00	0.00	0.00
Uvigerina peregrina	0.00	0.92	0.00	1.37	1.00	1.29	4.05	1.37	0.99	1.06	0.33	0.99	1.34	1.43	0.98	1.25	0.00	1.00	1.07	1.00	1.45	0.66	3.00	1.77
Uvigerina proboscidea	0.00	0.61	0.00	2.06	3.00	2.59	5.74	2.39	2.64	2.12	3.01	2.65	1.79	3.21	5.21	3.13	2.70	3.00	2.49	0.67	1.45	1.65	0.00	3.55
Uvigerina sp.	0.00	0.31	0.00	0.00	0.00	0.00	0.00	0.00	0.00	0.71	0.33	0.00	0.45	0.00	0.00	0.00	0.39	0.33	0.00	0.67	0.00	1.32	0.86	0.00
Valvulineria spp.	0.00	0.00	0.00	0.00	0.33	0.00	0.00	0.34	0.33	0.71	0.00	0.00	0.00	0.00	0.00	0.00	0.00	0.00	0.00	0.00	0.00	0.00	0.00	0.00
Vulvulina spinosa	0.34	0.61	0.58	0.34	0.33	0.65	0.00	0.34	0.66	1.06	1.00	1.32	2.23	0.71	0.65	0.94	1.54	0.33	0.00	0.67	0.73	0.00	0.43	0.00

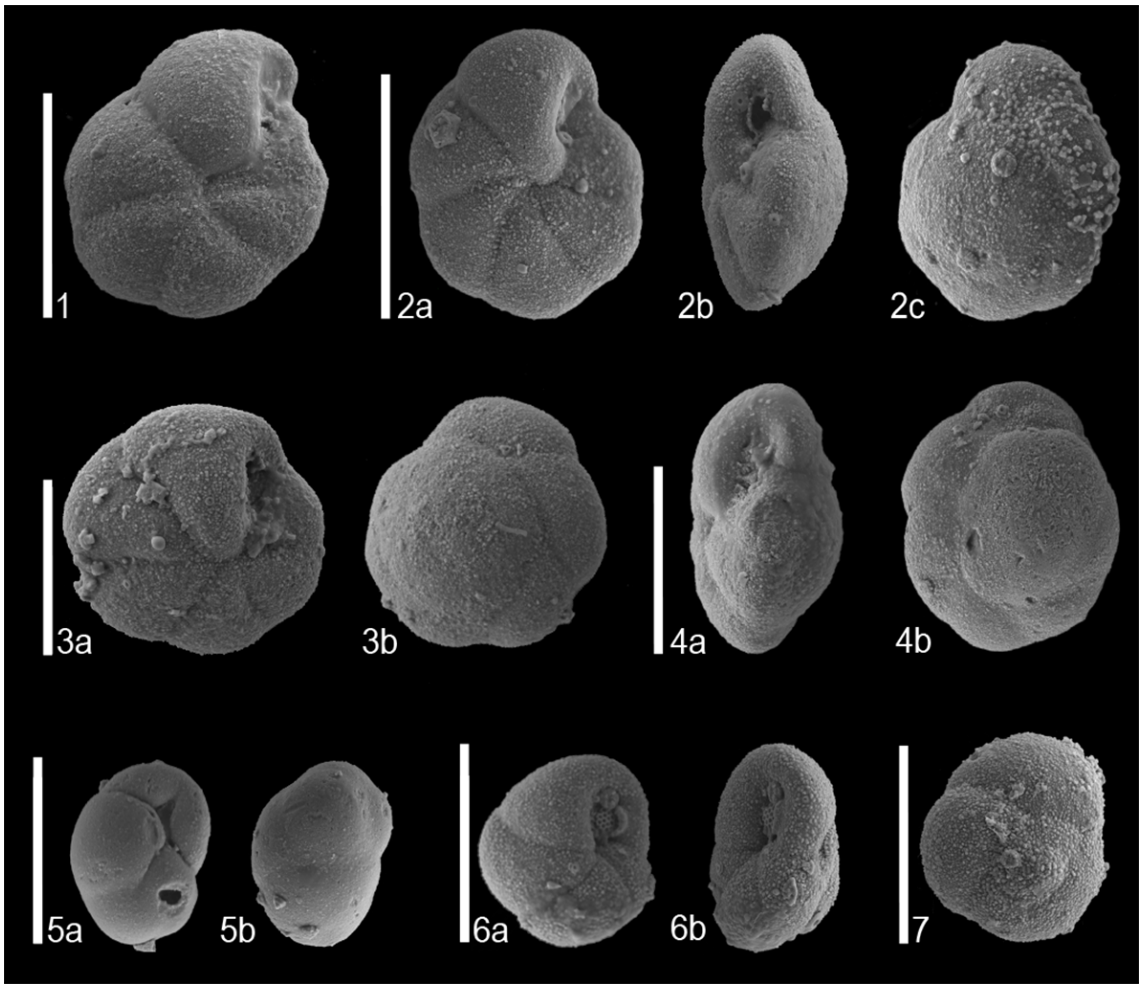

Plate 1. SEM images of selected benthic foraminiferal species at Site 1053. **(1)** *Pseudoparrella* sp. (MPZ-2023/386) ventral side. **(2)** *Pseudoparrella* sp. (MPZ-2023/387) **(a)** ventral side, **(b)** apertural view, and **(c)** dorsal side. **(3)** *Pseudoparrella* sp. (MPZ-2023/388) **(a)** ventral side and **(b)** dorsal side. **(4)** *Pseudoparrella* sp. (MPZ-2023/389) **(a)** apertural view and **(b)** dorsal side. **(5)** *Globocassidulina subglobosa* (MPZ-2023/390) **(a)** ventral side and **(b)** dorsal side. **(6)** *Cassidulina crassa* (MPZ-2023/391) **(a)** ventral side and **(b)** apertural view. **(7)** *Cassidulina crassa* (MPZ-2023/392) dorsal side. All scale bars represent 100 µm. All specimens were taken from sample 1053BH5 (11.5–12.5 cm) and are deposited in Museo de Ciencias Naturales de la Universidad de Zaragoza (MCNUZ).

the traditional CP15b biozone roughly corresponds to the upper CNE18 and CNE19 biozones of Agnini et al. (2014), allowing for further refinement of the age model.

Our new biostratigraphic data reveal that the base of *Reticulofenestra isabellae* – the marker for the base of biozone CNE19 – is present in the lowermost sample examined (sample no. 68; 75.20 rmcd) and that *R. reticulata* – the top common occurrence of which defines the base of CNE20 – is common throughout the study interval. This indicates that our entire depth profile (74.54–75.20 rmcd) falls within the CNE19 (*R. isabellae/R. reticulata* concurrent) nannofossil zone of the Priabonian, late Eocene (ca. 36 Ma; Agnini et al., 2014; Raffi et al., 2016).

3.2 Carbon and oxygen stable isotopes

Oxygen isotope values measured on bulk sediment ($\delta^{18}O_{bulk}$) range between 0.76 ‰ and −0.50 ‰ (Figs. 2, 3). A gradual trend towards more positive values can be observed from the bottom towards the top of the study interval. A prominent negative excursion (1 ‰) is recorded between 75.00 and 74.91 rmcd, with $\delta^{18}O_{bulk}$ values decreasing from 0.5 ‰ to −0.50 ‰. The peak of the negative excursion in $\delta^{18}O_{bulk}$ is recorded at 74.95 rmcd (Figs. 2, 3).

Carbon isotope values of bulk sediment ($\delta^{13}C_{bulk}$) range between 2.05 ‰ and 1.68 ‰ (Figs. 2, 3), and they show a general increasing trend towards the top of the studied interval. A 0.28 ‰ negative excursion is recorded between 75.00 and 74.91 rmcd. The minimum $\delta^{13}C_{bulk}$ value occurs

at 74.95 rmcd, coinciding with the peak of the negative excursion in $\delta^{18}O_{bulk}$ (Figs. 2, 3).

3.3 Benthic foraminiferal assemblages

Diversity (Fisher's α index) of the assemblages ranges between 6.17 (at 74.54 rmcd) and 14.71 (at 74.97 rmcd). High-diversity values (above an average Fisher's α index of 10.14) are more common between 75.03 and 74.94 rmcd (Fig. 3). The $H(S)$ values span between 1.39 (at 74.54 rmcd) and 2.56 (at 74.96 rmcd). Similar to the diversity, the lowest values are recorded in the uppermost sample, and high $H(S)$ values appear predominantly in the interval 74.99–74.91 rmcd (Fig. 3).

Benthic foraminiferal assemblages are strongly dominated by calcareous taxa, and agglutinated species make up only ~ 1.5 % of the assemblages. Taxa that occupy the substrate–water interface (epifaunal morphogroups) are generally more abundant than species that live deeper within the sediment (infaunal morphogroups) throughout the study interval, with relative abundances of epifaunal species ranging from 49.30 % to 74.45 % (Fig. 3). The epifaunal *Pseudoparrella* sp. strongly dominates the assemblages, with abundances that range between 27.44 % and 60.62 % (Fig. 2). The identification of this species is not straightforward, as it has similarities with other taxa that are common in the Eocene. *Pseudoparrella* sp. has a biconvex trochospiral test with an angular periphery, yet it is not carinated as in *Epistominella*. The wall is thin and smooth, and tests are characteristically very small (ca. 110–150 µm in diameter), more so than other similar genera like *Epistominella* and *Alabamina*. Two and a half to three tightly coiled whorls can be observed in the dorsal side. The dorsal sutures are straight to gently curved and strongly oblique, much more so than those of *Alabamina* and *Epistominella*. The ventral side is involute, with six to eight chambers in the last whorl separated by gently curved oblique sutures that turn almost radial near the closed umbilicus. The aperture is a narrow and straight interiomarginal slit in a subequatorial position, characteristic of the genus. It extends to the face of the last chamber on the umbilical side and is bordered by a narrow lip. Most of the individuals we observed display the characteristics mentioned above (Plate 1), which supports the accurate identification of *Pseudoparrella* sp. at ODP Site 1053. In addition to *Pseudoparrella*, the epifaunal genera *Cibicidoides*, *Nuttallinella*, *Gyroidinoides*, and *Anomalinoides* are common to abundant (Figs. 2, 3). Among infaunal taxa, buliminids s.l. (including *Uvigerina proboscidea* and *Uvigerina peregrina*), *Brizalina tectiformis* and *Globocassidulina subglobosa* are most abundant (Figs. 2, 3). To better analyse the evolution of the benthic foraminiferal assemblages, three intervals were identified based on the main trends in the $\delta^{18}O_{bulk}$ and $\delta^{13}C_{bulk}$ values (Figs. 2, 3).

Interval 1 (75.20 to 75.00 rmcd): heterogeneity and diversity of the assemblages are moderate in the lowermost sample of this interval (75.20 rmcd); they drop at 75.16 rmcd and then recover towards its upper part, reaching values of 2.15 and 11.85 at 75.04 and 75.03 rmcd (Fig. 3). Assemblages are dominated by epifaunal morphogroups which reach their absolute maximum (74.46 %) at 75.16 rmcd. *Pseudoparrella* sp. makes up 40.22 %–53.49 % of the assemblages. *Nuttallinella* sp. is common among epifaunal taxa, and *Nuttallides* sp., *Gyroidinoides* spp., *Cibicidoides* spp., and *Anomalinoides* spp. are present. The percentage of the epiphytic *Cibicides lobatulus* slightly increases (up to 4.06 %) across this interval. Infaunal morphogroups make up 25.5 %–39.7 % of the assemblages. Buliminids s.l. (including *Stainforthia* spp., *Uvigerina peregrina*, *U. proboscidea*, and *Pyramidina* spp.) and *Globocassidulina subglobosa* (Figs. 2, 3) are the most common taxa among infaunal morphogroups. The relative abundance of *Brizalina* spp. (including *Brizalina tectiformis*) increases up to 14.8 % towards the upper part of the interval.

Interval 2 (74.99 to 74.91 rmcd): the maximum diversity (14.71 at 74.97 rmcd) and heterogeneity (2.56 at 74.96 rmcd) of the assemblages is recorded in this interval, coinciding with the negative shifts in $\delta^{18}O_{bulk}$ and $\delta^{13}C_{bulk}$ and the maximum abundance of infaunal taxa such as *Globocassidulina subglobosa*, *Uvigerina proboscidea*, and *Bulimina* spp. (*B. alazanensis* and *B. elongata*). The infaunal *Brizalina* spp. (including *B. tectiformis*) make up to 13.95 % of the assemblages within this interval. The relative abundance of epifaunal morphogroups decreases in Interval 2, mostly due to the significant drop in percent *Pseudoparrella* sp. from 37.67 % at 74.99 rmcd to 27.44 % at 74.97 rmcd, followed by a gradual recovery towards the top of this interval. Coinciding with low values in percent *Pseudoparrella* sp., other epifaunal taxa such as *Anomalinoides* and *Cibicidoides* increase in relative abundance, making up 3.64 % and 8.37 % of the assemblages, respectively. *Nuttallinella* shows a similar trend, reaching a peak (9.93 % at 74.95 rmcd) slightly after the decrease in percent *Pseudoparrella* sp.

Interval 3 (74.90 to 74.54 rmcd): diversity and heterogeneity of the assemblages decrease across this interval, showing their minimum values in the uppermost sample. Epifaunal morphogroups dominate the assemblages (52.29 %–72.27 %). The percentage of *Pseudoparrella* sp. increases up-section, reaching its absolute maximum (60.61 %) in the uppermost part. *Cibicidoides* spp. (including *C. eocaenus*) and *Anomalinoides* are common among epifaunal taxa, and their relative abundance slightly decreases towards its top. The relative abundance of infaunal taxa slightly increases towards the upper half of Interval 3 (up to at 74.59 rmcd), mainly due to the increase in percent *Brizalina tectiformis*, *Bulimina alazanensis*, *Cassidulina crassa*, and *Globocassidulina subglobosa*, which reaches its highest abundance (11.54 %) across the studied section. The relative abundances of *Uvigerina proboscidea* and *Uvigerina peregrina* gradually decrease from the base to the top of Interval 3.

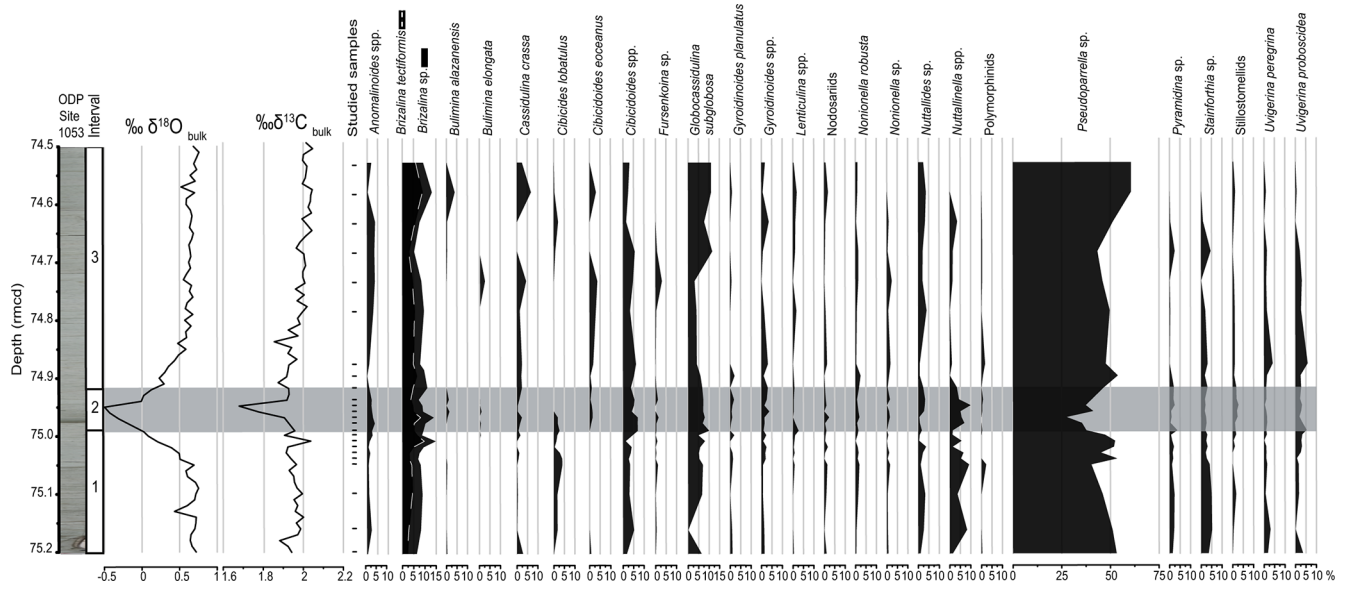

Figure 2. Bulk isotopic data and changes in the relative abundance of the benthic foraminiferal taxa that make up $> 2\,\%$ of the assemblages in at least one sample at Site 1053 plotted against depth (rmcd). The grey box highlights the interval that contains the negative excursions in $\delta^{13}C$ and $\delta^{18}O$.

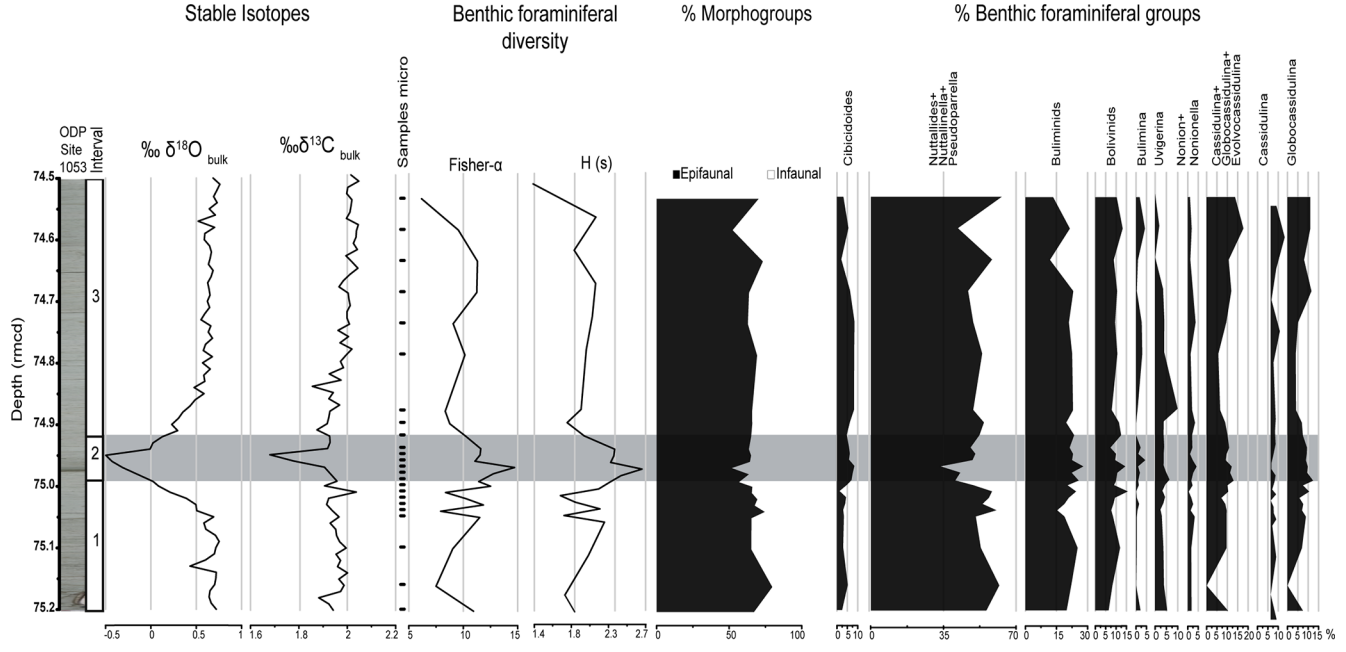

Figure 3. Bulk isotopic data from Site 1053 plotted against depth (rmcd). Benthic foraminiferal diversity and heterogeneity, morphogroups, and relative abundance of selected benthic foraminiferal taxa and groups. The grey box highlights the interval that contains the negative excursions in $\delta^{13}C$ and $\delta^{18}O$.

3.4 Calcareous nannofossil assemblages

Calcareous nannofossils are moderately to well preserved throughout the study interval. Prior to the isotopic excursions (75.20 to 75.00 rmcd; Interval 1), assemblages are relatively diverse and dominated by reticulofenestrids (particularly *Cyclicargolithus floridanus*, *Reticulofenestra minuta*, and *Reticulofenestra reticulata*), with common braarudosphaerids (*Pemma* spp., *Braarudosphaera* spp., *Micrantholithus* spp., and *Hexadelus* spp.), *Coccolithus pelagicus*, *Discoaster barbadiensis*, and *Umbilicosphaera* spp. and frequent to common *Coccolithus formosus*, *Discoaster saipanensis*, *Sphenolithus moriformis*, *Bramlettei serraculoides*,

and *Blackites* spp. Assemblage composition is fairly stable, with only minor fluctuations observed in the PCA results (samples almost entirely confined to values < 0 along both PCA dimensions 1 and 2; Fig. 4). Nevertheless, a major shift in nannofossil assemblage composition was identified at the onset of the paired carbon and oxygen isotope excursion (74.99 rmcd), Interval 2, as indicated by a large increase in the Dimension 1 PCA scores (Fig. 4). This shift is largely driven by the short-lived disappearance of almost all braarudosphaerids during Interval 2, as well as smaller, transient decreases in the abundances of *Discoaster tanii*, *Discoaster barbadiensis*, *Sphenolithus moriformis*, and *Helicosphaera* spp. and a slight increase in the relative abundance of *Pontosphaera* spp. (Fig. 4). A marked decrease in overall nannofossil abundance and a reduction in the cell size of most taxa accompany these assemblage changes, as well as an increase in the abundance of reworked taxa (particularly those of the Cretaceous age).

Assemblages in Interval 3 closely resemble those prior to the isotope excursions by 74.90 rmcd (Fig. 4). Braarudosphaerids reappear sequentially (*Pemma* → *Micrantholithus* → *Braarudosphaera*), but the abundance of *Micrantholithus* spp. does not return to previous values. Nannofossil community composition then remains relatively stable from 74.74 to 74.91 rmcd. Between 74.69 and 74.74 rmcd there is a second major shift in the nannoplankton community composition (albeit not as large as the first one), indicated by a modest increase in the Dimension 2 PCA scores (Fig. 4). Unlike the first event, this assemblage change does not appear to be connected to a carbon cycle perturbation and is predominantly driven by a slight decrease in the abundance of *Umbilicosphaera* spp. (particularly *U. bramlettei* and *U. detecta*) and *Helicosphaera* spp. and the brief disappearance of some sphenolith species (e.g. *S. apoxis*, *Furcatolithus predistentus*, and *S. pseudoradians*).

4 Palaeoenvironmental interpretation

4.1 Stable isotopes

The interpretation of the negative shift in $\delta^{18}O_{bulk}$ and $\delta^{13}C_{bulk}$ values across the study interval is not straightforward. If $\delta^{18}O_{bulk}$ values are interpreted in terms of palaeotemperature, the ~ 1 ‰ decrease in the uppermost part of Interval 1 and in Interval 2 may indicate a transient warming event followed by a return towards background conditions in Interval 3. The lowest $\delta^{18}O_{bulk}$ values coincide with a marked negative excursion in $\delta^{13}C_{bulk}$ within Interval 2. Changes in $\delta^{13}C$ are commonly related to perturbations of the global carbon cycle (e.g. biological productivity, ocean circulation, volcanic activity, burial and erosion of carbonate, atmospheric CO_2 concentrations, and enhanced ocean acidification; Wefer et al., 1999; Saltzman and Thomas, 2012; Greene et al., 2019; Zachos et al., 2005; Arreguín-Rodríguez and Alegret, 2022).

One might argue that the more negative carbon isotope values in our record might be related to methane seep, a mechanism that is common in the Blake Ridge area, at least since the latest Oligocene (Mountain and Toucholke, 1985; Borowski, 2004). If one speculates that methane seep was already active during the late Eocene, and that it reached the Blake Nose, then this mechanism might have caused diagenetic overprint on stable isotope ratios, specifically a decrease in $\delta^{13}C_{bulk}$ values. However, it has been documented that pore water affected by hydrate seep is enriched by around a 3 ‰ in ^{18}O relative to unaffected water (Hesse and Harrison, 1981; Ussler and Paull, 1995). This contribution of ^{18}O is linked to a decomposition of gas hydrates during carbonate precipitation that result in ^{18}O records affected by diagenetic overprint showing positive values relative to the VPDB standard (e.g. Pierre et al., 2012). We thus argue that it is unlikely that the negative shift in $\delta^{18}O_{bulk}$ was related to diagenetic overprint by methane seepage.

Coupled negative excursions in $\delta^{18}O_{bulk}$ and $\delta^{13}C_{bulk}$ are typically associated with hyperthermal events which are characterized by short-lived (tens to hundreds of kiloyears, kyr) perturbations of the global carbon cycle associated with warming in the atmosphere and across the water column, likely caused by the input of ^{13}C-depleted carbon into the ocean–atmosphere system (Thomas and Zachos, 2000; Zachos et al., 2010; Dickens, 2011). Since we were not able to analyse the isotopic signal of benthic foraminifera across the study interval at Site 1053, mostly due to the small size of the specimens and the amount of material required for the analyses, we cannot conclude that the event recorded in Interval 2 corresponds to a hyperthermal event. In addition, some of the consequences of other Paleogene hyperthermals, such as carbonate undersaturation and dissolution in deep-sea sediments or the proliferation of opportunistic benthic foraminifera (e.g. Jorissen et al., 2007; Alegret et al., 2010, 2021b; Arreguín-Rodríguez et al., 2018; Arreguín-Rodríguez and Alegret, 2022), have not been recorded at Site 1053.

We suggest that the negative excursions in $\delta^{18}O_{bulk}$ and $\delta^{13}C_{bulk}$ at Site 1053 were caused by regional rather than global changes (see Sect. 5), as previously suggested for the Blake Nose area during the late middle Eocene (Wade and Kroon, 2002; Okafor et al., 2009).

4.2 Benthic foraminiferal assemblages

The dominance of hyaline calcareous benthic foraminifera (> 98 %) over agglutinated taxa and the overall good preservation of the tests suggest that ODP Site 1053 was above the calcite compensation depth (CCD) during the Priabonian. No evidence has been identified that supports low oxygenation at this site (species tolerant to low-oxygen conditions do not dominate the assemblage). Moreover, the generalist species *Globocassidulina subglobosa* is present across the

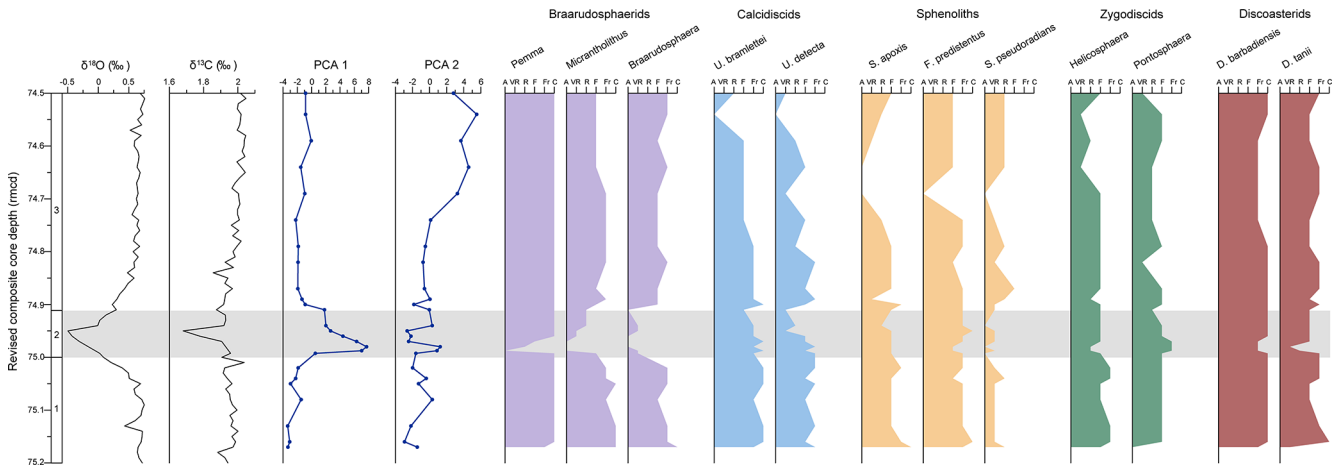

Figure 4. Bulk sediment δ^{18}O and δ^{13}C data from ODP Site 1053 plotted against depth (rmcd) are shown alongside the principal components analysis (PCA) axis 1 and axis 2 scores for calcareous nannofossil assemblages and the qualitative abundances of select nannofossil taxa. Contributions of each taxon with each PCA axis are based on their individual abundances in 10 fields of view. Genus abbreviations are as follows: U. is for *Umbilicosphaera*, S. is for *Sphenolithus*, F. is for *Furcatolithus*, and D. is for *Discoaster*.

whole study interval. This species has been linked to well-oxygenated bottom waters (Schönfeld, 2001; Martins et al., 2007; Singh and Gupta, 2010; Fenero et al., 2012), further supporting the idea that oxygen was not a limiting factor at Site 1053.

Overall, assemblages display moderate diversity and are dominated by the epifaunal *Pseudoparrella* sp. The genus *Pseudoparrella* is morphologically similar to *Epistominella*, which is abundant in oligotrophic bathyal settings where food supply is highly episodic (e.g. Schnitker, 1980; Gooday, 1986, 1996; Gooday and Hughes, 2002). Both genera have characteristic small and thin tests, smooth walls, and a moderate number of chambers. These traits are shared with other benthic foraminifera that feed predominantly on phytodetritus. These morphological characteristics are no mere convergence but rather reflect adaptations to their ecological niche and their ability to bloom upon organic fluxes (Gooday, 1993). We thus interpret the morphology of *Pseudoparrella* sp. as typical of the so-called phytodetritus-exploiting taxa (PET), a group of predominantly epifaunal, opportunistic taxa that bloom in response to pulses of phytodetritus (e.g. Gooday, 1993; Boscolo-Galazzo et al., 2015; Ortiz and Thomas, 2015; Rivero-Cuesta et al., 2019, 2020). In a similar way, living *Globocassidulina subglobosa* (Gooday, 1993, 1994) and *Cassidulina crassa* (Suhr et al., 2003; Suhr and Pond, 2006) have also been suggested to preferably feed on phytodetritus.

Benthic foraminiferal assemblages in Interval 1 show moderate diversity and heterogeneity. *Pseudoparrella* sp. is the main component of the assemblages (Fig. 2) and points to an intermittent delivery of fresh phytodetritus to the seafloor, which favoured its rapid reproduction and dominance over other epifaunal species. Its relative abundance decreased in Interval 2, which contains the negative shifts in bulk δ^{18}O and δ^{13}C (Fig. 2). We interpret this interval as indicative of a change in the amount of phytodetritus reaching the seafloor or in the periodicity of its supply, which may have favoured the diversity of benthic foraminiferal assemblages. The percentage of other epifaunal taxa such as *Nuttallinella*, *Cibicidoides*, or *Anomalinoides* increased across Interval 2, and the percentage of infaunal buliminids s.l. (e.g. *Brizalina tectiformis, Brizalina* sp., *Bulimina* sp., *Bulimina alazanensis*, and *Uvigerina proboscidea*; Fig. 2) also slightly increased (Fig. 3). Buliminids s.l. tend to flourish in low-oxygenation environments or in high-productivity conditions (e.g. Bernhard and San Gupta, 1999; Thomas et al., 2010; Fontanier et al., 2002). They are common throughout the study interval, but they do not dominate the assemblages, suggesting sustained mesotrophic conditions at Site 1053.

Diversity and heterogeneity of the assemblages decreased in Interval 3, reaching their minimum values at the top of the study interval, and the percentage of *Pseudoparrella* sp. increased up-section, showing its maximum abundance in the two uppermost samples (Fig. 2). Similarly, the relative abundance of *Globocassidulina subglobosa* increased upwards (Fig. 2), and the relative abundance of other epifaunal (e.g. *Nuttallinella* sp., *Cibicidoides* spp.; Fig. 2) and infaunal taxa decreased, suggesting the return to an enhanced supply of phytodetritus to the seafloor.

Phytodetritus exploiters are most commonly identified in the open ocean, where the flux of organic matter to the seafloor is not very high (e.g. Sun et al., 2006), and in mid- and high latitudes, where they have been described to live in phytodetritus aggregates (e.g. Gooday, 1993; Gooday and Hughes, 2002). At high latitudes, food supply to the seafloor is highly episodic (e.g. Smart et al., 1994) and linked to seasonal upwelling through the formation of a deep-mixing layer in winter that favours nutrient translocation and

large spring phytoplankton blooms (Sundby et al., 2016). Accordingly, PET are commonly used in fossil assemblages to identify periods of higher seasonality in food supply to the seafloor or pulsed deposition of phytodetritus (Smart et al., 1994; Thomas et al., 1995; Sun et al., 2006). PET have also been documented from sites located at tropical and subtropical latitudes during the Eocene (e.g. Boscolo-Galazzo et al., 2015). However, in the modern oceans, seasonal deep-winter mixing does not occur at these latitudes (Levitus et al., 1994a), and phytoplankton blooms are rather associated with irregular and patchy eddy activity (Bidigare et al., 2003; Dore et al., 2008). Intermittent eddies alter the pycnocline as they advance, producing phytoplankton blooms that can be intensified and prolonged via wind–eddy interactions (Dewar and Flierl, 1987; McGillicuddy et al., 2007).

One might argue that the changes in organic flux we inferred from our benthic foraminiferal assemblages during Interval 2 might be related to fluctuations in sediment transport intensity. This is the case for the Blake Ridge area, east of Blake Nose, where variations in the activity of the Deep Western Boundary Undercurrent (DWBUC) have been tied to fluctuations in the food supply to the local benthic foraminiferal communities during the Neogene (Mohan et al., 2011). If one speculates that the DWBUC was already active during the late Eocene and that the Blake Nose was on its depth and latitudinal range, then periods of intensified activity could have produced enhanced erosion in the Canadian continental shelf, transport, and eventually nutrient supply to the seafloor. In this case, benthic foraminiferal assemblages would be similar to those described by Mohan et al. (2011). Nevertheless, the dominance of *Pseudoparrella* sp. and the increase in other components of the assemblages during Interval 2, when the relative abundance of this taxon decreased, strongly suggest that phytodetritus was the principal food source of benthic foraminifera at Site 1053 and that changes in species composition mainly reflect a shift in its delivery. Phytodetritus is formed from the agglomeration of phytoplankton, and zooplankton remains in a gelatinous matrix, and it gradually settles towards the seafloor in a highly regional process (Rice et al., 1986; Riemann, 1989). We argue that benthic foraminiferal assemblages at Site 1053 reflect changes in the food supply on a regional scope rather than fluctuations in sediment transport from exogenous sources.

Moreover, DWBUC activity in the western North Atlantic is difficult to trace before Oligocene times (Tucholke and Mountain, 1986; Norris et al., 2012). The most consistent signal of DWBUC activity is the presence of a major unconformity through the upper Eocene–Oligocene strata along the North American eastern continental margin that is dated at ca. 28 Ma (Tucholke and Mountain, 1986). Tucholke and Mountain (1986) suggested that the Eirik and Gloria drifts south of Greenland, depositional structures linked to deep-boundary current activity, may have begun to grow in the middle Eocene, implying that a proto-DWBUC could have been already active during the middle Eocene. However, there is no evidence of DWBUC activity in the Blake Nose area at that time. Based on our calcareous nannofossil biostratigraphy, our record predates the most consistent evidence of DWBUC activity in Blake Nose by ca. 8 Ma.

4.3 Calcareous nannofossil assemblages

Overall, the consistently high abundance of nannofossil taxa such as *C. floridanus*, small *Reticulofenestra* spp. (see *R. minuta*), and braarudosphaerids, indicates a high nutrient (eutrophic) surface ocean throughout the study interval (e.g. Aubry, 1992; Kameo, 2002; Kelly et al., 2003; Auer et al., 2014; Ozdínová and Sotak, 2015; Kallanxhi et al., 2018). The presence of frequent to common *Discoaster* and *Sphenolithus* spp. suggests that these waters were also relatively warm (e.g. Aubry, 1992, 1998; Wei et al., 1992; Villa et al., 2014).

Braarudosphaerids, which are generally accepted to have an ecological preference for cooler, hyposaline, and eutrophic environments (e.g. Bukry, 1974; Kelly et al., 2003; Bartol et al., 2008; Auer et al., 2014; Liebrand et al., 2018; Kallanxhi et al., 2018), significantly decline at the onset of the carbon and oxygen isotopic excursions (Interval 2). It is unlikely that this decrease was caused by a reduction in surface ocean nutrients because the abundance of low-nutrient taxa (e.g. *Discoaster* spp.) also decreases, indicating the persistence of a eutrophic surface ocean. *Discoaster* spp. were also adapted to warmer waters, suggesting that the braarudosphaerid decline was not solely driven by the temperature increase identified in the $\delta^{18}O$ record. Instead, we speculate that the temporary decrease in braarudosphaerids during Interval 2 may represent decreased ocean stratification, with previous studies showing that *Braaurudosphaera* spp. tend to bloom when the water column is hyperstratified (Liebrand et al., 2018; Jones et al., 2021). This would have encouraged more mixing between the surface and deep ocean, an interpretation that is consistent with the observed increase in *Pontosphaera*, which may have been well adapted to nutrient mixing and turbulence (Kallanxhi et al., 2018). Alternatively, the decreased abundance of braarudosphaerids may suggest an increase in surface ocean salinity. This is supported by a slight decrease in the abundance of *Helicosphaera* (considered to be a hyposaline taxon; Flores et al., 2005; Wade and Bown, 2006; Narciso et al., 2010) and a slight increase in the abundance of *Pontosphaera*, which is potentially a hypersaline taxon (Bartol et al., 2008; Ozdínová and Sotak, 2015). However, this interpretation is very tentative due to inconsistencies in the reported palaeoecological preferences of both taxa (Kallanxhi et al., 2018). The increased abundance of reworked Cretaceous taxa coincident with the isotope excursions might indicate increased sediment transport and/or weathering during Interval 2. Nevertheless, they are overall rare, and it is unlikely that they are driving the observed changes in isotope values.

Between 74.74 and 74.69 rmcd, most sphenolith taxa (excluding *S. moriformis*) greatly decrease in abundance. As this assemblage change does not coincide with a carbon or oxygen isotope excursion, we speculate that it reflects a very brief, local change in the palaeoenvironment (e.g. a slight increase in surface ocean nutrients). Nannofossil assemblages within the topmost part of the study interval (74.69 to 74.50 rmcd) differ from those below 74.69 rmcd, as can be seen in the PCA results (Fig. 4). This dissimilarity is largely driven by decreased relative abundances of *Umbilicosphaera bramlettei*, *U. detecta*, and *Helicosphaera* spp. The palaeoecology of the genus *Umbilicosphaera* is uncertain but may be linked to warmer and/or more oligotrophic surface waters (Auer et al., 2014; Baumann et al., 2016), whereas *Helicosphaera* is generally thought to be best adapted to warm, eutrophic environments (e.g. Kallanxhi et al., 2018). Therefore, the decreased abundance of these two taxa may reflect the broad, gradual cooling trend that was reinstated after a brief interruption (as evidenced by the oxygen isotope record). Although this is not reflected by a similar decrease in the abundance of other warm-water taxa (e.g. *Sphenolithus* and *Discoaster* spp.) or an increase in cold-water taxa (e.g. *Chiasmolithus* spp. and *R. lockeri*; Villa et al., 2014), it is likely that our low-resolution qualitative approach simply does not detect the small shifts in nannofossil assemblages driven by such broad, gradual palaeoclimatic changes.

5 Discussion

At Site 1053, bulk $\delta^{18}O$ data show a negative shift of 1 ‰ in Interval 2. Changes of equal or greater amplitude have been repeatedly registered at Blake Nose during the late middle Eocene (Wade et al., 2000; Wade and Kroon, 2002; Okafor et al., 2009) and linked to regional phenomena. In a slightly older interval (39.8–38.2 Ma) at ODP Site 1051, Wade et al. (2000) associated transient ($\sim$ 100 kyr) shifts in $\delta^{18}O$ of > 1 ‰ to an episodic reduction in the thermal structure linked to variations in the upwelling intensity. Wade et al. (2001) expanded on that work by analysing a longer sequence at the same site (42.40–39.55 Ma). Their data reinforce the idea that fluctuations in the upwelling intensity may have caused high-amplitude, short-term fluctuations in the oxygen stable isotope record (0.9 ‰ in 50–100 kyr) at Site 1051, not fully disregarding the possibility that changes in surface ocean salinity were also reflected in their $\delta^{18}O$ data.

Furthermore, Wade and Kroon (2002) examined a younger sequence (39.6–37.9 Ma) from ODP Site 1052 and proposed that the pronounced variability in $\delta^{18}O$ data reflects a highly variable regional oceanographic system, most probably related to a longitudinal displacement of the Gulf Stream affecting Blake Nose, fluctuations in upwelling intensity, or a combination of both processes. Okafor et al. (2009) performed a high-resolution analysis on a 400 kyr long sequence (37.9–37.5 Ma) from Site 1052. They concluded that the high-amplitude variability in $\delta^{18}O$ records (1.4 ‰ in 2.5–4 kyr) reflects a combination of changes in sea surface temperature and the $\delta^{18}O$ of the regional seawater. These changes cannot be explained by an increase in continental ice and rather point to a combination of an enhanced influence of the Gulf Stream over Blake Nose and an overall weakening of the hydrological cycle.

The longitudinal displacement of the proto-Gulf Stream (Okafor et al., 2009) could account for the bulk isotope record and microfossil assemblages at Site 1053 (Fig. 5). The flow of the proto-Gulf Stream eastward may have exposed Site 1053 to its associated eddies during Interval 1. The net movement of water outwards, characteristic of cyclonic eddies in the Northern Hemisphere, depresses the pycnocline and induces downwelling (Fuglister, 1972; McGillicuddy et al., 2007). An intermittent transit of cyclonic eddies could have enhanced stratification, allowing braarudosphaerids to bloom in the surface ocean and inducing the flux of phytodetritus to the seafloor. Calcareous nannoplankton contribute to the marine biological pump both directly by their role in the sequestration and sinking of dissolved inorganic carbon and indirectly by delivering ballast material derived from their tests (Gibbs et al., 2018; Griffith et al., 2021). Braarudosphaerids tend to be more heavily calcified than other nannoplankton groups due to their uniquely laminated plates (Gibbs et al., 2018; Liebrand et al., 2018).

Moreover, Liebrand et al. (2018) noted that periods of increased accumulation of *Braarudosphaera* in the South Atlantic Ocean (ODP Site 1264) during the Oligocene positively correlated with enhanced stratification and export flux towards the seafloor. It is possible that the same mechanism was at play in Blake Nose, and that the coccospheres of *Braarudosphaera* improved the ballasting of phytodetritus, ultimately favouring the proliferation of *Pseudoparrella* sp. among benthic foraminifera during Interval 1.

A drift of the proto-Gulf Stream westwards during Interval 2 may have left Site 1053 out of the influence zone of its eddies, without which the depressed pycnocline would return to its basal state, enhancing layer mixing through the water column. This would explain the increase in *Pontosphaera* during Interval 2, the substantial decline in braarudosphaerids, and a resulting decline in the phytodetritus flux to the seafloor, accounting for the decrease in percent *Pseudoparrella* sp. The input of warmer, nutrient-depleted surface waters in the area would account for the negative excursions in $\delta^{18}O_{bulk}$ and $\delta^{13}C_{bulk}$ and the contemporaneous decrease in nannoplankton productivity. Western boundary currents are known to have a different salinity signature from the surrounding waters (e.g. Levitus et al., 1994a, b), so it is plausible that the brief alteration of the surface ocean salinity inferred from the nannofossil record could also indicate a greater impact of the proto-Gulf Stream over Site 1053. An eastward shift in the proto-Gulf Stream during Interval 3 and the return of its eddies could account for the return to

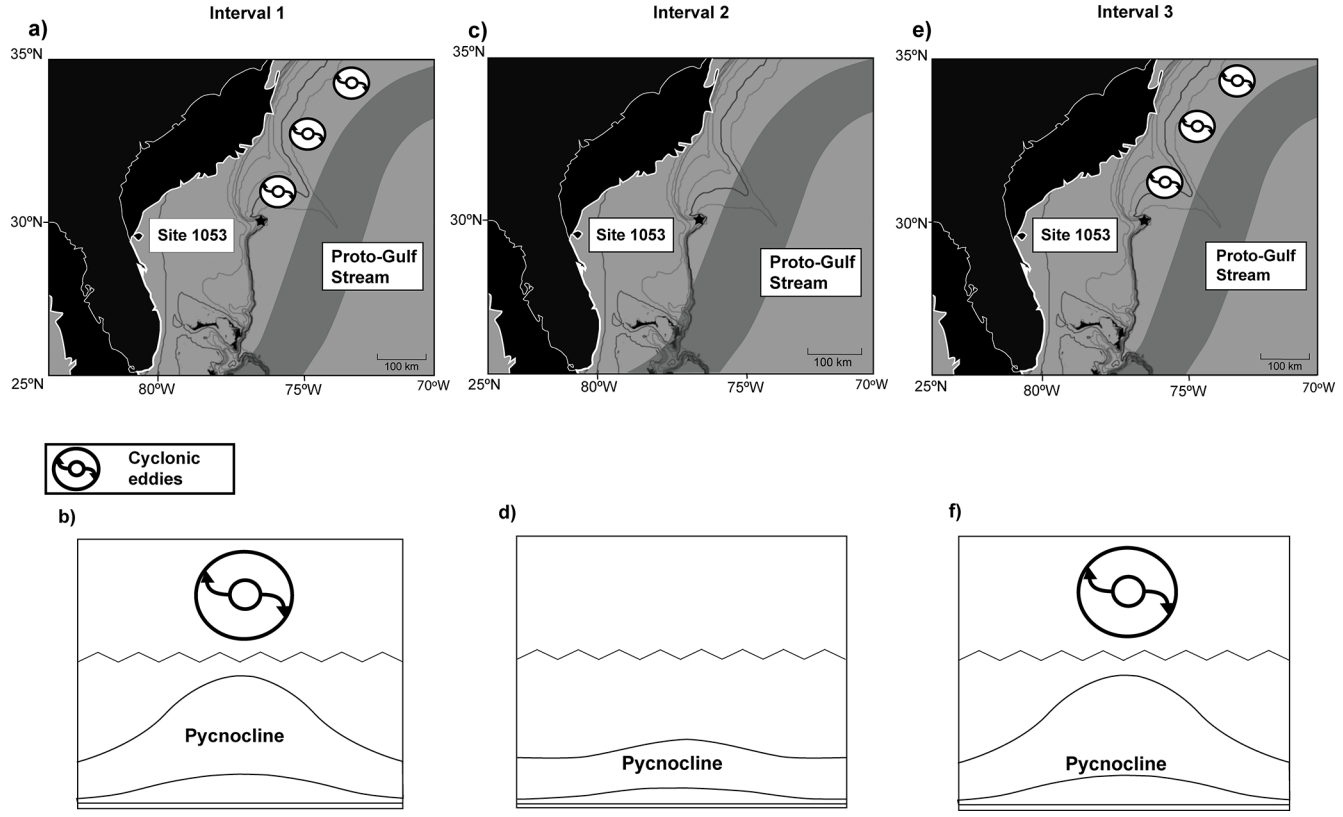

Figure 5. Distribution of the proto-Gulf Stream and its associated eddies during the three intervals identified at ODP Site 1053 **(a, c, e)** and water column with and without the influence of cyclonic eddies **(b–d–f)**. Maps **(a, c, e)** modified from the late Eocene (ca. 36 Ma) PALEOMAP from PaleoAtlas for GPlates (Scotese, 2016, and Norris et al., 1998). Thick and thin white outlines represent the coastline of the Florida peninsula during the late Eocene (ca. 36 Ma) and at present, respectively. Longitude and latitude are present-day coordinates.

previous palaeoceanographic conditions with microfossil assemblages similar to those from Interval 1.

An intensified transit of anticyclonic eddies during Interval 2 could also explain the loss of water column structure inferred from our micropaleontological records since this type of eddy is known to induce layer mixing (e.g. Witkowski et al., 2021). However, they also enhance primary production by pumping nutrient-rich deep water upwards (e.g. Roughan et al., 2017). Therefore, if anticyclonic eddies had affected Site 1053 during Interval 2, then not only the input of nutrient-rich colder water should have been registered as a positive trend in our $\delta^{18}O_{bulk}$ and $\delta^{13}C_{bulk}$ isotope records, but calcareous nannofossil assemblages should have reflected increased productivity at that moment. Not only do our stable isotope data show the opposing trend, but calcareous nannofossil assemblages decrease slightly in size and overall abundance during Interval 2.

Longitudinal shifts in the distribution of the proto-Gulf Stream and its associated eddy activity have been proposed for the Blake Nose area during the middle to late middle Eocene (42.2–37.3 Ma). Moreover, it has been observed that the Gulf Stream can alter its distribution on a decadal scale in response to larger-scale oceanographic phenomena like the Atlantic Meridional Overturning Circulation (AMOC) and the North Atlantic Oscillation (Sanchez-Franks and Zhang, 2015). This supports the idea that the proto-Gulf Stream could have altered its path several times, even in such a short time span as the one we describe here. Intermittent warm-water and/or transient eddy input have been linked to high-amplitude SST fluctuations registered in the oxygen isotope (e.g. Wade et al., 2000) and calcareous nannofossil records (Newsam et al., 2017; Wade and Kroon, 2002), as well as to Mg-/Ca-derived palaeotemperature reconstructions (Okafor et al., 2009) and biosiliceous accumulation records (Witkowski et al., 2021).

Based on our micropaleontological and stable isotope data, we suggest a similar mechanism for the study interval at ODP site 1053. While we acknowledge that our palaeoenvironmental interpretation is limited by the lack of stable isotope data on benthic foraminifera, our results from Site 1053 offer valuable insights into the faunal, floral, and palaeoceanographic turnover across a short interval of the Priabonian in the subtropical North Atlantic. In addition, our benthic foraminiferal data contribute to fill the gap in the Paleogene diversity curve of the Atlantic Ocean and suggest that diversity in the western North Atlantic was lower than in

the southeast Atlantic during the Priabonian (Alegret et al., 2021a). Further quantitative studies of benthic foraminiferal assemblages across a longer time interval will contribute to assessing the evolution of this group in the Atlantic Ocean since the middle Eocene, which is when the latitudinal diversity gradient was established (Alegret et al., 2021a).

6 Conclusions

We carried out an integrated geochemical (stable isotopes) and micropaleontological study of a 70 cm thick, late Eocene interval from ODP Site 1053 on Blake Nose (western North Atlantic Ocean). Calcareous nannofossil biostratigraphy places the study interval within the CNE19 zone of the Priabonian (ca. 36 Ma). To further investigate an intriguing coupled negative $\delta^{13}C$ and $\delta^{18}O$ excursion that was recognized in the bulk sediment record, we carried out detailed assemblage studies on benthic foraminifera and calcareous nannofossils and characterized three distinct palaeoecological intervals. Intervals 1 and 3 consist of diverse and stable nannofossil assemblages and moderate-diversity benthic assemblages dominated by the phytodetritus-exploiting taxon *Pseudoparrella* sp. These intervals are associated with high surface ocean productivity, a colder and well-stratified water column, and increased fluxes of phytodetritus to the seafloor. Interval 2, which contains the $\delta^{13}C$ and $\delta^{18}O$ excursion, is characterized by less diverse calcareous nannoplankton assemblages that show a transient – yet significant – decline in the high-productivity braarudosphaerid group. In contrast, benthic foraminiferal assemblages become more diverse, and the dominance of *Pseudoparrella* sp. decreases. These features suggest that Interval 2 was characterized by warmer surface waters, lower surface ocean productivity, higher layer mixing in the water column, and a weaker flux of phytodetritus to the seafloor compared to Intervals 1 and 3.

We argue that the palaeoceanographic conditions inferred during Interval 2 could result from a brief input of warm, nutrient-depleted water into the Blake Nose area, linked to a displacement of the proto-Gulf Stream towards the area of study, which would account for the decrease in stratification and in the delivery of phytodetritus to the seafloor. We hypothesize that the proto-Gulf Stream shifted its course eastwards during Interval 3, restoring the previous palaeoceanographic conditions. Our results are consistent with prior interpretations on the Blake Nose area, which occupies a key role in the understanding of the proto-Gulf Stream and its dynamics during the Paleogene.

Data availability. Underlying data are available in the Supplement and from the PANGAEA database at https://doi.pangaea.de/10.1594/PANGAEA.965594 (De Entrambasaguas et al., 2024).

Supplement. The supplement related to this article is available online at: https://doi.org/10.5194/jm-43-303-2024-supplement.

Author contributions. LA and TW conceived the study. TW, JdE, LA, and HLJ processed the samples. TW performed the isotope analyses. LA and JdE analysed benthic foraminifera and HJ the calcareous nannofossils. JdE wrote and edited the article under the supervision of LA. HLJ participated in the writing of the article. All authors interpreted the results and edited the article.

Competing interests. At least one of the (co-)authors is a member of the editorial board of *Journal of Micropalaeontology*. The peer-review process was guided by an independent editor, and the authors also have no other competing interests to declare.

Disclaimer. Publisher's note: Copernicus Publications remains neutral with regard to jurisdictional claims made in the text, published maps, institutional affiliations, or any other geographical representation in this paper. While Copernicus Publications makes every effort to include appropriate place names, the final responsibility lies with the authors.

Acknowledgements. This study has received financial support from MCIN/AEI/10.13039/501100011033 (grant no. PID2019-105537RB-I00) and "ERDF A way of making Europe". This research used samples and data provided by the International Ocean Discovery Program (IODP). The authors would like to acknowledge the use of Servicio General de Apoyo a la Investigación – SAI, Universidad de Zaragoza. We thank Ellen Thomas, for advice on the identification of *Pseudoparrella* sp., and Henning Kuhnert and his team, for stable isotope analyses at MARUM. Funding for this research has also been provided by the Deutsche Forschungsgemeinschaft (DFG, German Research Foundation), under Germany's Excellence Strategy (EXC-2077), to Thomas Westerhold and Heather L. Jones (grant. no. 390741603) and to Thomas Westerhold (grant no. 320221997).

Financial support. This research has been supported by the Spanish Ministry of Science and Innovation (MCIN/AEI/10.13039/501 10001 1033 505; grant no. PID2019-105537RB-100), by "ERDF A way of making Europe", and by the Deutsche Forschungsgemeinschaft (EXC-2077; grant nos. 390741603 and 320221997).

Review statement. This paper was edited by Sev Kender and reviewed by Eiichi Setoyama and two anonymous referees.

References

Agnini, C., Fornaciari, E., Raffi, I., Catanzariti, R., Pälike, H., Backman, J., and Rio, D.: Biozonation and biochronology of Paleogene calcareous nannofossils from low and middle latitudes, Newsl. Stratigr., 47, 131–181, https://doi.org/10.1127/0078-0421/2014/0042, 2014.

Agnostou, E., John, E. H., Edgar, K. M., Foster, G. L., Ridgwell, A., Inglis, G. N., Pancost, R. D., Lunt, D. J., and Pearson, P. N.: Changing atmospheric CO_2 concentration was the primary driver of early Cenozoic climate, Nature, 533, 380–384, https://doi.org/10.1038/nature17423, 2016.

Alegret, L. and Thomas, E.: Benthic foraminifera across the Cretaceous/Paleogene boundary in the Southern Ocean (ODP Site 690): diversity, food and carbonate saturation, Mar. Micropaleontol., 105, 40–51, https://doi.org/10.1130/B30055.1, 2013.

Alegret, L., Ortiz, S., Arenillas, I., and Molina, E.: What happens when the ocean is overheated? The foraminiferal response across the Paleocene-Eocene Thermal Maximum at the Alamedilla section (Spain), Geol. Soc. Am. Bull., 122, 1616–1624, https://doi.org/10.1130/B30055.1, 2010.

Alegret, L., Arreguín-Rodríguez, G. J., Trasviña-Moreno, C. A., and Thomas, E.: Turnover and stability in the deep sea: benthic foraminifera as tracers of Paleogene global change, Global Planet. Change, 196, 103372, https://doi.org/10.1016/j.gloplacha.2020.103372, 2021a.

Alegret, L., Harper, D. T., Agnini, C., Newsham, C., Westerhold, T., Cramwinckel, M. J., Dallanave, E., Dickens, G. R., and Sutherland, R.: Biotic Response to early Eocene Warming Events: Integrated Record from Offshore Zealandia, north Tasman Sea, Paleoceanogr. Paleocl., 36, e2020PA004179, https://doi.org/10.1029/2020PA004179, 2021b.

Arreguín-Rodríguez, G. J. and Alegret, L.: Deep-sea benthic foraminiferal turnover across early Eocene hyperthermal events at Northeast Atlantic DSDP Site 550, Palaeogeogr. Palaeocl., 451, 62–72, https://doi.org/10.1016/j.palaeo.2016.03.010, 2022.

Arreguín-Rodríguez, G. J., Thomas, E., D'haenens, S., Speijer, R. P., and Alegret, L.: Early Eocene deep-sea benthic faunas: recovery in globally warm oceans, PLoS One, 13, e0193167, https://doi.org/10.1371/journal.pone.0193167, 2018.

Aubry, M. P.: Late Paleogene calcareous nannoplankton evolution: A tale of climatic deterioration, in: Eocene–Oligocene climatic and biotic evolution, edited by: Prothero, D. R. and Berggren, W. A., Princeton University Press, 272–309, https://doi.org/10.1515/9781400862924.272, 1992.

Aubry, M. P.: Early Paleogene calcareous nannoplankton evolution: a tale of climatic amelioration, in: Late Paleocene and Early Eocene Climatic and Biotic Evolution, edited by: Aubry, M. P., Lucas, S., and Berggren, W. A., Columbia University Press, New York, 158–203, 1998.

Auer, G., Piller, W. E., and Harzhauser, M.: High-resolution calcareous nannoplankton palaeoecology as a proxy for small-scale environmental changes in the Early Miocene, Mar. Micropaleontol., 111, 53–65, https://doi.org/10.1016/j.marmicro.2014.06.005, 2014.

Bartol, M., Pavšič, J., Dobnikar, M., and Bernasconi, S. M.: Unusual Braarudosphaera bigelowii and Micrantholithus vesper enrichment in the Early Miocene sediments from the Slovenian Corridor, a seaway linking the Central Paratethys and the Mediterranean, Palaeogeogr. Palaeocl., 267, 77–88, https://doi.org/10.1016/j.palaeo.2008.06.005, 2008.

Baumann, K. H., Saavedra-Pellitero, M., Böckel, B., and Ott, C.: Morphometry, biogeography and ecology of Calcidiscus and Umbilicosphaera in the South Atlantic, Revue de Micropaléontologie, 59, 239–251, https://doi.org/10.1016/j.revmic.2016.03.001, 2016.

Bernhard, J. M. and San Gupta, B. K.: Foraminifera of oxygen-depleted environments, in: Modern foraminifera, Springer, Dordrecht, 201–216, https://doi.org/10.1007/0-306-48104-9_12, 1999.

Bice, K. L., Scotese, C. R., Seidov, D., and Barron, E. J.: Quantifying the role of geographic change in Cenozoic ocean heat transport using uncoupled atmosphere and ocean models, Palaeogeogr. Palaeocl., 161, 295–310, https://doi.org/10.1016/S0031-0182(00)00072-9, 2000.

Bidigare, R. R., Benitez-Nelson, C., Leonard, C. L., Quay, P. D., Parsons, M. L., Foley, D. G., and Seki, M. P.: Influence of a cyclonic eddy on microheterotroph biomass and carbon export in the lee of Hawaii, Geophys. Res. Lett., 30, 1318, https://doi.org/10.1029/2002GL016393, 2003.

Billett, D. M. S., Lampitt, R. S., Rice, A. L., and Mantoura, R. F. C.: Seasonal sedimentation of phytoplankton to the deep-sea benthos, Nature, 302, 520–522, 1983.

Boersma, A., Premoli Silva, I., and Shackleton, N. J.: Atlantic Eocene planktonic foraminiferal paleohydrographic indicators and stable isotope paleoceanography, Paleoceanography, 2, 287–331, https://doi.org/10.1029/PA002i003p00287, 1987.

Borrelli, C., Cramer, B. S., and Katz, M. E.: Bipolar Atlantic deep-water circulation in the middle-late Eocene: Effects of Southern Ocean gateway openings, Paleoceanography, 29, 308–327, https://doi.org/10.1002/2012PA002444, 2014.

Borrelli, C., Katz, M. E., and Toggweiler, J. R.: Middle to late Eocene changes of the ocean carbonate cycle, Paleoceanogr. Paleocl., 36, e2020PA004168, https://doi.org/10.1029/2020PA004168, 2021.

Borowski, W.: A review of methane and gas hydrates in the dynamic, stratified system of the Blake Ridge region, offshore southeastern North America, Chem. Geol., 205, 311–346, 2004.

Boscolo-Galazzo, F. B., Thomas, E., and Giusberti, L.: Benthic foraminiferal response to the Middle Eocene climatic optimum (MECO) in the south-eastern Atlantic (ODP Site 1263), Palaeogeogr. Palaeocl., 417, 432–444, https://doi.org/10.1016/j.palaeo.2014.10.004, 2015.

Bouchet, V. M., Sauriau, P. G., Debenay, J. P., Mermillod-Blondin, F., Schmidt, S., Amiard, J. C., and Dupas, B.: Influence of the mode of macrofauna-mediated bioturbation on the vertical distribution of living benthic foraminifera: first insight from axial tomodensitometry, J. Exp. Mar. Biol. Ecol., 371, 20–33, 2009.

Bown, P. R. and Young, J. R.: Techniques, in: Calcareous Nannofossil Biostratigraphy, edited by: Bown, P. R., Dordrecht, the Netherlands, Kluwer Academic Publishing, 16–28, https://doi.org/10.1007/978-94-011-4902-0_2, 1998.

Bukry, D.: Coccoliths as paleosalinity indicators: evidence from the Black Sea, AAPG Memoir, 20, 303–327, https://doi.org/10.1306/M20377C2, 1974.

Cramer, B. S., Toggweiler, J. R., Wright, J. D., Katz, M. E., and Miller, K. G.: Ocean overturning since the Late Cretaceous: Inferences from a new benthic foraminiferal

isotope compilation, Paleoceanography, 24, PA4216, https://doi.org/10.1029/2008PA001683, 2009.

Cramwinckel, M. J., Huber, M., Kocken, I. J., Agnini, C., Bijl, P. K., Bohaty, S. M., Frieling, J., Goldner, A., Hilgen, F. J., Kip, E. L., Petersen, F., van der Ploeg, R., Röhl, U., Schouten, S., and Sluijs, A.: Synchronous tropical and polar temperature evolution in the Eocene, Nature, 559, 382–386, https://doi.org/10.1038/s41586-018-0272-2, 2018.

Corliss, B. H.: Microhabitats of benthic foraminifera within deep-sea sediments, Nature, 314, 435–438, https://doi.org/10.1038/314435a0, 1985.

Corliss, B. H. and Chen, C.: Morphotype patterns of Norwegian Sea deep-sea benthic foraminifera and ecological implications, Geology, 16, 716–719, https://doi.org/10.1130/0091-7613(1988)016<0716:MPONSD>2.3.CO;2, 1988.

De Entrambasaguas, J., Westerhold, T., Jones, H., and Alegret, L.: Stable isotopes of benthic foraminifera and calcareous nannofossils from ODP Site 171-1053, PANGAEA [data set], https://doi.org/10.1594/PANGAEA.965594, 2024.

Dewar, W. K. and Flierl, G. R.: Some effects of the wind on rings, J. Phys. Oceanogr., 17, 1653–1667, https://doi.org/10.1175/1520-0485(1987)017<1653:SEOTWO>2.0.CO;2, 1987.

Dickens, G. R.: Down the Rabbit Hole: toward appropriate discussion of methane release from gas hydrate systems during the Paleocene-Eocene thermal maximum and other past hyperthermal events, Clim. Past, 7, 831–846, https://doi.org/10.5194/cp-7-831-2011, 2011.

Dore, J. E., Letelier, R. M., Church, M. J., Lukas, R., and Karl, D. M.: Summer phytoplankton blooms in the oligotrophic North Pacific Subtropical gyre: historical perspective and recent observations, Prog. Oceanogr., 76, 2–38, https://doi.org/10.1016/j.pocean.2007.10.002, 2008.

Fenero, R., Thomas, E., Alegret, L., and Molina, E.: Evolución paleoambiental del tránsito Eoceno-Oligoceno en el Atlántico Sur (Sondeo 1263) basada en foraminíferos bentonicos, Geogaceta, 49, 3–6, 2010.

Fenero, R., Thomas, E., Alegret, L., and Molina, E.: Oligocene benthic foraminifera from the Fuente Caldera section (Spain, western Tethys): taxonomy and paleoenvironmental inferences, J. Foramin. Res., 42, 286–304, https://doi.org/10.2113/gsjfr.42.4.286, 2012.

Flores, J. A., Sierro, F. J., Filippelli, G. M., Bárcena, M. Á., Pérez-Folgado, M., Vázquez, A., and Utrilla, R.: Surface water dynamics and phytoplankton communities during deposition of cyclic late Messinian sapropel sequences in the western Mediterranean, Mar. Micropaleontol., 56, 50–79, https://doi.org/10.1016/j.marmicro.2005.04.002, 2005.

Fontanier, C., Jorissen, F. J., Licari, L., Alexandre, A., Anschutz, P., and Carbonel, P.: Live benthic foraminiferal faunas from the Bay of Biscay: faunal density, composition, and microhabitats, Deep-Sea Res. Pt. I, 49, 751–785, https://doi.org/10.1016/S0967-0637(01)00078-4, 2002.

Fuglister, F. C.: Cyclonic rings formed by the Gulf Stream 1965–1966, in: Studies in Physical Oceanography: A tribute to George Wust on His 80th Birthday, edited by: Gordon, A., 137–168, Gordon and Breach, New York, 1972.

Gibbs, S. J., Sheward, R. M., Bown, P. R., Poulton, A. J., and Alvarez, S. A.: Warm plankton soup and red herrings: calcareous nannoplankton cellular communities and the Palaeocene–Eocene Thermal Maximum, Philos. T. R. Soc. A., 376, 20170075, https://doi.org/10.1098/rsta.2017.0075, 2018.

Gooday, A. J.: Meiofaunal foraminiferans from the bathyal Pocupine Seabight (Northeast Atlantic): size structure, standing crop, taxonomic composition, species diversity and vertical distribution in the sediment, Deep-Sea Res., 33, 1345–1373, 1986.

Gooday, A. J.: Deep-sea benthic foraminiferal species which exploit phytodetritus: characteristic features and controls on distribution, Mar. Micropaleontol., 22, 187–205, https://doi.org/10.1016/0377-8398(93)90043-W, 1993.

Gooday, A. J.: The biology of deep-sea foraminifera: a review of some advances and their applications in paleoceanography, Palaios, 9, 14–31, https://doi.org/10.2307/3515075, 1994.

Gooday, A. J.: Epifaunal and shallow infaunal foraminiferal communities at three abyssal NE Atlantic sites subject to differing phytodetritus input regimes, Deep-Sea Res., 43, 1395–1421, 1996.

Gooday, A. J. and Hughes, J. A.: Foraminifera associated with phytodetritus deposits at a bathyal site in the northern Rockall Trough (NE Atlantic): seasonal contrasts and a comparison of stained and dead assemblages, Mar. Micropaleontol., 46, 83–110, https://doi.org/10.1016/S0377-8398(02)00050-6, 2002.

Gooday, A. J. and Turley, C. M.: Responses by benthic organisms to inputs of organic material to the ocean floor: a review, Philos. T. R. Soc. A., 331, 119–138, https://doi.org/10.1098/rsta.1990.0060, 1990.

Gordon, A. L.: The role of thermohaline circulation in global climate change, Lamont-Doherty Geological Observatory 1990 and 1991 Report, Lamont-Doherty Earth Observatory Technical Report, 44–51, https://doi.org/10.7916/D8M04G8H 1991.

Greene, S. E., Ridgwell, A., Kirtland-Turner, S., Schmidt, D. N., Pälike, H., Thomas, E., Greene, L. K., and Hoogakker, B. A. A.: Early Cenozoic decoupling of climate and carbonate compensation depth trends, Paleoceanogr. Paleocl., 34, 930–945, https://doi.org/10.1029/2019PA003601, 2019.

Griffith, E. M., Thomas, E., Lewis, A. R., Penman, D. E., Westerhold, T., and Winguth, A. M. E.: Bentho-Pelagic decoupling: The marine biological carbon pump during Eocene hyperthermals, Paleoceanogr. Paleocl., 36, e2020PA004053, https://doi.org/10.1029/2020PA004053, 2021.

Guernet, C. and Bellier, J. P.: Ostracodes paléocènes et éocènes du blake nose (Leg ODP 171B) et évolution des environnements bathyaux au large de la Floride, Revue de Micropaléontologie, 43, 249–279, https://doi.org/10.1016/S0035-1598(00)90140-5, 2000.

Hesse, R. and Harrison, W. E.: Gas hydrates (clathrates) causing porewater freshening and oxygen isotope fractionation in deep-water sedimentary sections of terrigenous continental margins, Earth. Planet. Sc. Lett., 55, 453–462, 1981.

Holbourn, A., Henderson, A. S., and MacLeod, N.: Atlas of benthic foraminifera, John Wiley and Sons, https://doi.org/10.1002/9781118452493, 2013.

Hotinski, R. M. and Toggweiler, J. R.: Impact of a Tethyan circumglobal passage on ocean heat transport and "equable" climates, Paleoceanography, 18, 1007, https://doi.org/10.1029/2001PA000730, 2003.

Huber, M. and Sloan, L. C.: Climatic responses to tropical sea surface temperature changes on a "greenhouse" Earth, Paleoceanog-

raphy, 15, 443–450, https://doi.org/10.1029/1999PA000455, 2000.

Hutchinson, D. K., de Boer, A. M., Coxall, H. K., Caballero, R., Nilsson, J., and Baatsen, M.: Climate sensitivity and meridional overturning circulation in the late Eocene using GFDL CM2.1, Clim. Past, 14, 789–810, https://doi.org/10.5194/cp-14-789-2018, 2018.

Jones, H. L., Scrobola, Z., and Bralower, T. J.: Size and shape variation in the calcareous nannoplankton genus Braarudosphaera following the Cretaceous/Paleogene (K/Pg) mass extinction: clues as to its evolutionary success, Paleobiology, 47, 680–703, https://doi.org/10.1017/pab.2021.15, 2021.

Jorissen, F. J. and Wittling, I.: Ecological evidence from livedead comparisons of benthic foraminiferal faunas off Cape Blanc (Northwest Africa), Palaeogeogr. Palaeocl., 149, 151–170, https://doi.org/10.1016/S0031-0182(98)00198-9, 1999.

Jorissen, F. J., de Stigter, H. C., and Widmark, J. G.: A conceptual model explaining benthic foraminiferal microhabitats, Mar. Micropaleontol., 26, 3–15, https://doi.org/10.1016/0377-8398(95)00047-X, 1995.

Jorissen, F. J., Fontanier, C., and Thomas, E.: Paleoceanographical proxies based on deep-sea benthic foraminiferal assemblage characteristics, in: Proxies in Late Cenozoic Paleoceanography: Pt. 2: Biological tracers and biomarkers, edited by: Hillaire-Marcel, C. and de Vernal, A., Elsevier, 263–326, https://doi.org/10.1016/S1572-5480(07)01012-3, 2007.

Kallanxhi, M. E., Bălc, R., Ćorić, S., Székely, S. F., and Filipescu, S.: The Rupelian–Chattian transition in the northwestern Transylvanian Basin (Romania) revealed by calcareous nannofossils: implications for biostratigraphy and palaeoenvironmental reconstruction, Geol. Carpath., 69, 264–282, https://doi.org/10.1515/geoca-2018-0016, 2018.

Kameo, K.: Late Pliocene Caribbean surface water dynamics and climatic changes based on calcareous nannofossil records, Palaeogeogr. Palaeocl., 179, 211–226, https://doi.org/10.1016/S0031-0182(01)00432-1, 2002.

Kamikuri, S. and Wade, B. S.: Radiolarian magnetobiochronology and faunal turnover across the middle/late Eocene boundary at Ocean Drilling Program Site 1052 in the western North Atlantic Ocean, Mar. Micropaleontol., 88–89, 41–53, https://doi.org/10.1016/j.marmicro.2012.03.001, 2012.

Kassambara, A. and Mundt, F.: factoextra: Extract and Visualize the Results of Multivariate Data Analyses, R package version 1.0.7, https://cran.r-project.org/web/packages/factoextra/ (last access: April 2023), 2020.

Katz, M. E., Cramer, B. S., Toggweiler, J. R., Esmay, G., Liu, C., Miller, K. G., Rosenthal, Y., Wade, B. S., and Wright, J. D.: Impact of Antarctic Circumpolar Current development on late Paleogene ocean structure, Science, 332, 1076–1079, https://doi.org/10.1126/science.1202122, 2011.

Kelly, D. C., Norris, R. D., and Zachos, J. C.: Deciphering the paleoceanographic significance of Early Oligocene Braarudosphaera chalks in the South Atlantic, Mar. Micropaleontol., 49, 49–63, https://doi.org/10.1016/S0377-8398(03)00027-6, 2003.

Kroon, D., Norris, R. D., Klaus, A., the ODP Leg 171B Shipboard Scientific Party: Drilling Blake Nose: the search for evidence of extreme Palaeogene–Cretaceous climates and extraterrestrial events, Geol. Today, 171B, 222–226, 1998.

Lear, C. H., Elderfield, H., and Wilson, P. A.: Cenozoic deep-sea temperatures and global ice volumes from Mg/Ca in benthic foraminiferal calcite, Science, 287, 269–272, https://doi.org/10.1126/science.287.5451.269, 2000.

Levitus, S., Burgett, R., and Boyer, T. P.: World Ocean Atlas 1994, vol. 3, Salinity, NOAA Atlas NESDIS, 111 pp., NOAA, Silver Spring, Md, https://repository.library.noaa.gov/view/noaa/1382 (last access: April 2023), 1994a.

Levitus, S., Antonov, J., and Boyer, T. P.: Interannual variability of temperature at a depth of 125 m in the North Atlantic Ocean, Science, 266, 96–99, https://doi.org/10.1126/science.266.5182.96, 1994b.

Liebrand, D., Raffi, I., Fraguas, Á., Laxenaire, R., Bosmans, J. H., Hilgen, F. J., Wilson, P. A., Batenburg, S. J., Beddow, H. M., Bohaty, S. M., and Bown, P. R.: Orbitally forced hyperstratification of the Oligocene South Atlantic Ocean, Paleoceanogr. Paleoclimatol., 33, 511–529, https://doi.org/10.1002/2017PA003222, 2018.

Loeblich, A. R. and Tappan, H.: Foraminiferal genera and their classification, 2 vols., Van Nostrand Reinhold, New York, 1182 pp., 1987.

Mallon, J., Glock, N., and Schonfeld, J.: The response of benthic foraminifera to low oxygen conditions of the Peruvian oxygen minimum zone, in: Anoxia, Springer, Dordrecht, 305–321, https://doi.org/10.1007/978-94-007-1896-8_16, 2012.

Martins, V., Dubert, J., Jouanneau, J.-M., Weber, O., Ferreira da Silva, E., Patinha, C., Alveirinho Días, J. M., and Rohca, F.: A multiproxy approach of the Holocene evolution of shelf–slope circulation on the NW Iberian Continental Shelf, Mar. Geol., 239, 1–18, https://doi.org/10.1016/j.margeo.2006.11.001, 2007.

McGillicuddy Jr., D. J., Anderson, L. A., Bates, N. R., Bibby, T., Buesseler, K. O., Carlson, C. A., Davis, C. S., Ewart, C., Falkowski, P. G., Goldthwait, S. A., Hansell, D. A., Jenkins, W. J., Johnson, R., Kosnyrev, V. K., Ledwell, J. R., Li, Q. P., Siegel, D. A., and Steinberg, D. K.: Eddy/wind interactions stimulate extraordinary mid-ocean plankton blooms, Science, 316, 1021–1026, https://doi.org/10.1126/science.1136256, 2007.

Mohan, K., Gupta, A. K., and Bhaumik, A. K.: Distribution of deep-sea benthic foraminifera in the Neogene of Blake Ridge, NW Atlantic Ocean, J. Micropalaeontol., 30, 33–74, https://doi.org/10.1144/0262-821X10-008, 2011.

Mountain, G. S. and Tucholke, B. E.: Mesozoic and Cenozoic geology of the U.S. continental slope and rise, in: Geologic Evolution of the United States Atlantic Margin, edited by: Poag, C. W., Van Nostrand-Reinhold, New York, 293–341, ISBN 978-0442273064, 1985.

Murphy, C. H.: Blake Plateau. South Carolina Encyclopedia, University of South Carolina, Institute for Southern Studies, https://www.scencyclopedia.org/sce/entries/blake-plateau/ (last access: 5 August 2023), 1995.

Murray, J. W.: Ecology and applications of benthic foraminifera, Cambridge University Press, https://doi.org/10.1017/CBO9780511535529, 2006.

Narciso, Á., Flores, J. A., Cachão, M., Javier Sierro, F., Colmenero-Hidalgo, E., Piva, A., and Asioli, A.: Sea surface dynamics and coccolithophore behaviour during sapropel deposition of Marine Isotope Stages 7, 6 and 5 in Western Adriatic sea, Rev. Esp. Micropaleontol., 42, 345–358, 2010.

Norris, R. D., Kroon, D., Klaus, A., and the scientists from expedition 171B: Site 1053, in: Proc. ODP, Init. Repts., 171B, College Station, TX (Ocean Drilling Program), edited by: Norris, R. D., Kroon, D., and Klaus, A.,321–348, https://doi.org/10.2973/odp.proc.ir.171b.107.1998, 1998.

Norris, R. D., Wilson, P. A., Blum, P., and Expedition 342 Scientists: Paleogene Newfoundland sediment drifts and MDHDS test, in: Procc IODP (Vol. 342), College Station, Integrated Ocean Drilling Program, 2012.

Newsam, C., Bown, P. R., Wade, B. S., and Jones, H. L.: Muted calcareous nannoplankton response at the Middle/Late Eocene Turnover event in the western North Atlantic, Newsl. Stratigr., 50, 297–309, https://doi.org/10.1127/nos/2016/0306, 2017.

Okada, H. and Bukry, D.: Supplementary modification and introduction of code numbers to the low-latitude coccolith biostratigraphic zonation (Bukry, 1973; 1975), Mar. Micropalaeontol., 5, 321–325, https://doi.org/10.1016/0377-8398(80)90016-X, 1980.

Okafor, C. U., Thomas, D. J., Wade, B. S., and Firth, J.: Environmental change in the subtropics during the late middle Eocene greenhouse and global implications, Geochem. Geophy. Geosy., 10, Q07003, https://doi.org/10.1029/2009GC002450, 2009.

Ortiz, S. and Thomas, E.: Deep-sea benthic foraminiferal turnover during the early–middle Eocene transition at Walvis Ridge (SE Atlantic), Palaeogeogr. Palaeocl., 417, 126–136, https://doi.org/10.1016/j.palaeo.2014.10.023, 2015.

Ozdínová, S. and Soták, J.: Oligocene-Early Miocene planktonic microbiostratigraphy and paleoenvironments of the South Slovakian Basin (Lucenec Depression), Geol. Carpath., 65, 451–470, https://doi.org/10.1515/geoca-2015-0005, 2015.

Paull, C. K. and Dillon, W. P.: Structure, stratigraphy, and geologic history of the Florida-Hatteras shelf and inner Blake Plateau, AAPG Bull., 64, 339–358, https://doi.org/10.1306/2F919404-16CE-11D7-8645000102C1865D, 1980.

Pierre, C., Blanc-Vallleron, M. M., Demange, J., Boudouma, O., Foucher, J. P., Pape, T., Himmler, T., Fakete, N., and Spiess, V.: Authigenic carbonates from active methane seeps offshore southwest Africa, Geo-Mar. Lett., 32, 501–513, 2012.

Pinet, P. R., Popenoe, P., and Nelligan, D. F.: Gulf Stream: Reconstruction of Cenozoic flow patterns over the Blake Plateau, Geology, 9, 266–270, https://doi.org/10.1130/0091-7613(1981)9<266:GSROCF>2.0.CO;2, 1981.

Raffi, I., Agnini, C., Backman, J., Catanzariti, R., and Pälike, H.: A Cenozoic calcareous nannofossil biozonation from low and middle latitudes: A synthesis, J. Nano. Res., 36, 121–132, https://doi.org/10.58998/jnr2206, 2016.

Rice, A. L., Billett, D. S. M., Fry, J., John, A. W. G., Lampitt, R. S., Mantoura, R. F. C., and Morris, R. J.: Seasonal deposition of phytodetritus to the deep-sea floor, P. Roy. Soc. Edinb. B., 88, 265–279, https://doi.org/10.1017/S0269727000004590, 1986.

Richardson, P. L.: Gulf stream rings, in: Eddies in Marine Science, Robinson, A. R., 19–45, Springer, Berlin, ISBN 978-3-642-69005-1, 1983.

Riemann, F.: Gelatinous phytoplankton detritus aggregates on the Atlantic deep-sea bed. Structure and mode of formation, Mar. Biol., 100, 533–539, 1989.

Rivero-Cuesta, L., Westerhold, T., Agnini, C., Dallanave, E., Wilkens, R. H., and Alegret, L.: Paleoenvironmental changes at ODP Site 702 (South Atlantic): anatomy of the middle eocene climatic optimum, Paleoceanogr. Paleoclimatol., 34, 2047–2066, https://doi.org/10.1029/2019PA003806, 2019.

Rivero-Cuesta, L., Westerhold, T., and Alegret, L.: The Late Lutetian Thermal Maximum (middle Eocene): first record of deep-sea benthic foraminiferal response, Palaeogeogr. Palaeocl., 545, 109637, https://doi.org/10.1016/j.palaeo.2020.109637, 2020.

Roughan, M., Keating, S. R., Schaeffer, A., Heredia, C. P., Rocha, C., Griffin, D., Robertson, R., and Suthers, I. M.: A tale of two eddies: The biophysical characteristics of two contrasting cyclonic eddies in the East Australian Current System, J. Geophys. Res.-Oceans, 122, 2494–2518, https://doi.org/10.1002/2016JC012241, 2017.

Saltzman, M. R. and Thomas, E.: Carbon isotope stratigraphy, in: The Geologic Time Scale, edited by: Gradstein, F. M., Ogg, J. G., Schmitz, M., and Ogg, G., Elsevier, 207–232, https://doi.org/10.1016/B978-0-444-59425-9.00011-1, 2012.

Sanchez-Franks, A. and Zhang, R.: Impact of the Atlantic meridional overturning circulation on the decadal variability of the Gulf Stream path and regional chlorophyll and nutrient concentrations, Geophys. Res. Lett., 42, 9889–9897, https://doi.org/10.1002/2015GL066262, 2015.

Schlagintweit, F. and Enos, P.: Uppermost Jurassic? – Neocomian shallow-water carbonates of the Blake Nose, USA: DsDp site 392a revisited, Acta Palaeontologica Romaniae, 9, 39–56, 2013.

Schnitker, D.: Quaternary deep-sea benthic foraminifers and water masses, Annu. Rev. Earth Pl. Sc., 8, 343–370, 1980.

Scotese, C. R.: PALEOMAP PaleoAtlas for GPlates and the PaleoData Plotter Program, PALEOMAP Project, https://www.earthbyte.org/paleomap-paleoatlas-for-gplates/ (last access: March 2023), 2016.

Schönfeld, J.: Benthic foraminifera and pore-water oxygen profiles: a re-assessment of species boundary conditions at the western Iberian margin, J. Foramin. Res., 31, 86–107, https://doi.org/10.2113/0310086, 2001.

Singh, R. K. and Gupta, A. K.: Deep-sea benthic foraminiferal changes in the eastern Indian Ocean (ODP Hole 757B): Their links to deep Indonesian (Pacific) flow and high latitude glaciation during the Neogene, Episodes, 33, 74–82, https://doi.org/10.18814/epiiugs/2010/v33i2/001, 2010.

Singh, D. P., Saraswat, R., and Nigam, R: Untangling the effect of organic matter and dissolved oxygen on living benthic foraminifera in the southeastern Arabian Sea, Mar. Pollut. Bull., 172, 112883, https://doi.org/10.1016/j.marpolbul.2021.112883, 2021.

Smart, C. W., King, S. C., Gooday, A. J., Murray, J. W., and Thomas, E.: A benthic foraminiferal proxy of pulsed organic matter paleofluxes, Mar. Micropaleontol., 23, 89–99, https://doi.org/10.1016/0377-8398(94)90002-7, 1994.

Sun, X., Corliss, B. H., Brown, C. W., and Showers, W. J.: The effect of primary productivity and seasonality on the distribution of deep-sea benthic foraminifera in the North Atlantic, Deep-Sea Res. Pt. I, 53, 28–47, https://doi.org/10.1016/j.dsr.2005.07.003, 2006.

Sundby, S., Drinkwater, K. F., and Kjesbu, O. S.: The North Atlantic spring-bloom system-Where the changing climate meets the winter dark, Front. Mar. Sci., 3, 28, https://doi.org/10.3389/fmars.2016.00028, 2016.

Suhr, S. B. and Pond, D. W.: Antarctic benthic foraminifera facilitate rapid cycling of phytoplankton-derived or-

ganic carbon, Deep-Sea Res. Pt. II, 53, 895–902, https://doi.org/10.1016/j.dsr2.2006.02.002, 2006.

Suhr, S. B., Pond, D. W., Gooday, A. J., and Smith, C. R.: Selective feeding by benthic foraminifera on phytodetritus on the western Antarctic Peninsula shelf: evidence from fatty acid biomarker analysis, Mar. Ecol.-Prog. Ser., 262, 153–162, https://doi.org/10.3354/meps262153, 2003.

Thiel, H., Pfannkuche, O., Schriever, G., Lochte, K., Gooday, A. J., Hemleben, C. C., Mantoura, R. F. C., Turley, C. M., Patching, J. W., and Riemann, F.: Phytodetritus on the deep-sea floor in a central oceanic region of the Northeast Atlantic, Biol. Oceanogr., 6, 203–239, 1989.

Thomas, E. and Zachos, J. C.: Was the late Paleocene thermal maximum a unique event?, GFF, 122, 169–170, https://doi.org/10.1080/11035890001221169, 2000.

Thomas, E., Booth, L., Maslin, M., and Shackleton, N. J.: Northeastern Atlantic benthic foraminifera during the last 45,000 years: changes in productivity seen from the bottom up, Paleoceanography, 10, 545–562, https://doi.org/10.1029/94PA03056, 1995.

Thomas, E., Zachos, J. C., Bralower, T. J., Huber, B., MacLeod, K., and Wing, S.: Deep-sea environments on a warm earth: latest Paleocene-early Eocene, in: Warm Climates in Earth History, edited by: Huber, B. T., Macleod, K. G., and Wing, S. L., Division III Faculty Publications, Cambridge University Press, Cambridge, 132–160, 2010.

Tucholke, B. E. and Moutain, G. S.: Tertiary palaeoceanography of the western North Atlantic, in: The Western North Atlantic Region, Volume M: The Geology of North America, edited by: Vogt, P. and Tucholke, B., Geological Society of America, Boulder, CO, https://doi.org/10.1130/DNAG-GNA-M.631, 1986.

Ussler III, W. and Paull, C. K.: Effects of ion exclusion and isotopic fractionation on pore water geochemistry during gas hydrate formation and decomposition, Geo-Mar. Lett., 15, 37–44, https://doi.org/10.1007/BF01204496, 1995.

Van Morkhoven, F. M., Berggren, W. A., and Edwards, A. S.: Cenozoic cosmopolitan deep-water benthic foraminifera, B. Cent. Rech. Expl., 18, 90–91, https://doi.org/10.2113/gsjfr.18.1.90, 1986.

Van Mourik, C. A., Brinkhuis, H., and Williams, G. L.: Mid-to Late Eocene organic-walled dinoflagellate cysts from ODP Leg 171B, offshore Florida, Geol. Soc. Lond. Spec. Pub., 183, 225–251, https://doi.org/10.1144/GSL.SP.2001.183.01.11, 2001.

Villa, G., Fioroni, C., Persico, D., Roberts, A. P., and Florindo, F.: Middle Eocene to Late Oligocene Antarctic glaciation/deglaciation and southern ocean productivity, Paleoceanography, 29, 223–237, https://doi.org/10.1002/2013PA002518, 2014.

Wade, B. S. and Bown, P. R.: Calcareous nannofossils in extreme environments: the Messinian salinity crisis, Polemi Basin, Cyprus, Palaeogeogr. Palaeocl., 233, 271–286, https://doi.org/10.1016/j.palaeo.2005.10.007, 2006.

Wade, B. S. and Kroon, D.: Middle Eocene regional climate instability: Evidence from the western North Atlantic, Geology, 30, 1011–1014, https://doi.org/10.1130/0091-7613(2002)030<1011:MERCIE>2.0.CO;2, 2002.

Wade, B. S., Kroon, D., and Norris, R. D.: Upwelling in the late middle Eocene at Blake Nose?, GFF, 122, 174–175, https://doi.org/10.1080/11035890001221174, 2000.

Wade, B. S., Kroon, D., and Norris, R. D.: Orbitally forced climate change in the late middle Eocene at Blake Nose (Leg 171B): Evidence from stable isotopes, in Western North Atlantic Palaeogene and Cretaceous Palaeoceanography Foraminifera, edited by: Kroon, D., Norris, R. D., and Klaus, A., Geological Society Special Publications, 183, 273–291, https://doi.org/10.1144/GSL.SP.2001.183.01.13, 2001.

Watkins, D. K. and Self-Trail, J. M.: Calcareous nannofossil evidence for the existence of the Gulf Stream during the late Maastrichtian, Paleoceanography, 20, PA3006, https://doi.org/10.1029/2004PA001121, 2005.

Wefer, G., Berger, W. H., Bijma, J., and Fischer, G.: Clues to ocean history: A brief overview of proxies, in: Use of Proxies in Paleoceanography: Examples from the South Atlantic, edited by: Fischer, G. and Wefer, G., Springer-Verlagsexpertise, 1–68, https://doi.org/10.1007/978-3-642-58646-0_1, 1999.

Westerhold, T., Marwan, N., Drury, A. J., Liebrand, D., Agnini, C., Anagnostou, E., Barnet, J. S. K., Bohaty, S. M., De Vleeschouwer, D., Florindo, F., Frederichs, T., Hodell, D. A., Holbourn, A. E., Kroon, D., Lauretano, V., Littler, K., Lourens, L. J., Lyle, M., Pälike, H., Röhl, U., Tian, J., Wilkens, R. H., Wilson, P. A., and Zachos, J. C.: An astronomically dated record of Earth's climate and its predictability over the last 66 million years, Science, 369, 1383–1387, https://doi.org/10.1126/science.aba6853, 2020.

Wei, W., Villa, G., and Wise, S. W.: Paleoceanographic implications of Eocene-Oligocene calcareous nannofossils from Sites 711 and 748 in the Indian Ocean. Proc. Ocean Drilling Program, Sci. Res., 120, 979–999, https://doi.org/10.2973/odp.proc.sr.120.199.1992, 1992.

Witkowski, J., Bryłka, K., Bohaty, S. M., Mydłowska, E., Penman, D. E., and Wade, B. S.: North Atlantic marine biogenic silica accumulation through the early to middle Paleogene: implications for ocean circulation and silicate weathering feedback, Clim. Past, 17, 1937–1954, https://doi.org/10.5194/cp-17-1937-2021, 2021.

Young, J. R., Bown, P. R., and Lees, J. A.: Nannotax3 website, International Nannoplankton Association, https://www.mikrotax.org/Nannotax3, last access: 21 April 2022.

Zachos, J., Stott, L. D., and Lohmann, K. C.: Evolution of the early Cenozoic marine temperatures, Paleoceanography, 9, 3153–387, https://doi.org/10.1029/93PA03266, 1994.

Zachos, J. C., Röhl, U., Schellenberg, S. A., Sluijs, A., Hodell, D. A., Kelly, D. C., Thomas, E., Nicolo, M., Raffi, I., Lourens, L. J., McCarren, H., and Kroon, D.: Rapid acidification of the ocean during the Paleocene-Eocene thermal Maximum, Science, 308, 1611–1615, https://doi.org/10.1126/science.1109004, 2005.

Zachos, J. C., McCarren, H., Murphy, B., Röhl, U., and Westerhold, T.: Tempo and scale of late Paleocene and early Eocene carbon isotope cycles: implications for the origin of hyperthermals, Earth Planet. Sc. Lett., 299, 242–249, https://doi.org/10.1016/j.epsl.2010.09.004, 2010.